

AD-A128 732

ANALYSIS OF BARKHAUSEN NOISE TO ASSESS SHRINK FIT
STRESSES(U) SOUTHWEST RESEARCH INST SAN ANTONIO TX
W D PERRY ET AL. FEB 81 SWRI-15-5607-805

1/1

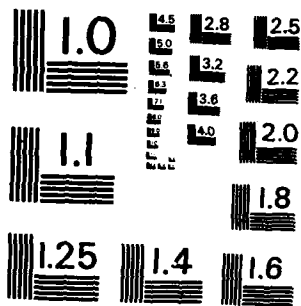
UNCLASSIFIED

DLA900-79-C-1266

F/G 11/6

NL

END
FILE
FORM
7 82



MICROCOPY RESOLUTION TEST CHART
 NATIONAL BUREAU OF STANDARDS-1963-A

AD A 128732

DTIC FILE COPY

SECURITY CLASSIFICATION OF THIS PAGE (When Data Entered)

REPORT DOCUMENTATION PAGE		READ INSTRUCTIONS BEFORE COMPLETING FORM								
1. REPORT NUMBER	2. GOVT ACCESSION NO. AD A128732	3. RECIPIENT'S CATALOG NUMBER								
4. TITLE (and Subtitle) Analysis of Barkhausen Noise to Assess Shrink Fit Stresses		5. TYPE OF REPORT & PERIOD COVERED Final Report								
7. AUTHOR(s) W. D. Perry J. R. Barton		6. PERFORMING ORG. REPORT NUMBER SWRI 15-5607-805								
9. PERFORMING ORGANIZATION NAME AND ADDRESS Southwest Research Institute 8500 Culebra Road, P.O. Drawer 28510 San Antonio, Texas 78284		8. CONTRACT OR GRANT NUMBER(s) DLA 900-79-C-1266								
11. CONTROLLING OFFICE NAME AND ADDRESS U.S. Army Aviation Research and Development Command St. Louis, Missouri		10. PROGRAM ELEMENT, PROJECT, TASK AREA & WORK UNIT NUMBERS								
14. MONITORING AGENCY NAME & ADDRESS (if different from Controlling Office)		12. REPORT DATE February 1981								
		13. NUMBER OF PAGES 42								
		15. SECURITY CLASS. (of this report) Unclassified								
		15a. DECLASSIFICATION/DOWNGRADING SCHEDULE								
16. DISTRIBUTION STATEMENT (of this Report) Approved for public release; distribution unlimited.										
17. DISTRIBUTION STATEMENT (of the abstract entered in Block 20, if different from Report)										
18. SUPPLEMENTARY NOTES										
19. KEY WORDS (Continue on reverse side if necessary and identify by block number) <table border="0"> <tr> <td>Nondestructive testing</td> <td>Thermal Interference fit</td> </tr> <tr> <td>Residual Stress</td> <td>Bushings</td> </tr> <tr> <td>Barkhausen effect</td> <td>Shrink Fit</td> </tr> <tr> <td>Ferromagnetic materials</td> <td></td> </tr> </table>			Nondestructive testing	Thermal Interference fit	Residual Stress	Bushings	Barkhausen effect	Shrink Fit	Ferromagnetic materials	
Nondestructive testing	Thermal Interference fit									
Residual Stress	Bushings									
Barkhausen effect	Shrink Fit									
Ferromagnetic materials										
20. ABSTRACT (Continue on reverse side if necessary and identify by block number) <p>The possible application of Barkhausen Noise Analysis to assess shrink fit stresses in steel bushings was investigated. Ten specimens of four different size NAS steel bushings were used in experiments to determine the relationship between the Barkhausen signal amplitude and the hoop-stress in the bushings. This relationship was investigated for specimens which were loaded by a simple clamping fixture and specimens subjected to actual thermal interference fits. The results show that while the relationship of Barkhausen</p>										

DTIC ELECTE
MAY 31 1983

DD FORM 1 JAN 73 1473

EDITION OF 1 NOV 65 IS OBSOLETE

Unclassified
SECURITY CLASSIFICATION OF THIS PAGE (When Data Entered)

signal amplitude to hoop stress is predictable for specimens loaded by the simple clamping fixture, the relationship was less predictable for actual thermal fit bushings. The variation in results could possibly be due to variable levels of axial stress produced by the differential thermal expansion of the steel and aluminum.

91



Accession For	
NIS GRA&I	<input checked="" type="checkbox"/>
ERIC IAP	<input type="checkbox"/>
Unannounced	<input type="checkbox"/>
Justification	
By	
Distribution	
Availability Codes	
Avail and/or	
Dist	Special
A	

Unclassified

TABLE OF CONTENTS

	<u>Page</u>
LIST OF ILLUSTRATIONS	iv
LIST OF TABLES	v
I. INTRODUCTION	1
II. SUMMARY	3
III. ANALYSIS OF STRESSES PRODUCED BY THERMAL FITS	5
IV. SPECIMENS AND EQUIPMENT	8
V. EXPERIMENTS	13
VI. CONCLUSIONS	34
VII. RECOMMENDATIONS	35
VIII. REFERENCES	36
APPENDIX A - CALCULATION OF HOOP STRESS PRODUCED BY A THERMAL INTERFERENCE FIT	

LIST OF ILLUSTRATIONS

<u>FIGURE</u>	<u>TITLE</u>	<u>PAGE</u>
1	Helicopter Drag Strut Assembly	2
2	Calculated Range of Interference at 400°F Differential Temperature for each Bushing Diameter	7
3	Simple Fixture for Applying Stress to Bushings	10
4	Aluminum Test Specimen and Bushing Before and After Assembly	11
5	Equipment Used in This Investigation	12
6	Loading Fixture Showing Measurement Locations on a Split Bushing	14
7	Barkhausen Signal Amplitude Versus Applied Hoop Stress at Location "A"	15
8	Barkhausen Signal Amplitude Versus Applied Hoop Stress at Location "B"	16
9	Barkhausen Signal Amplitude Versus Applied Hoop Stress at 0.5 Hx and 1.0 Hz Magnetization Frequency	18
10	Barkhausen Signal Amplitude Versus Specimen Number Showing Amplitude Variations Caused by Residual Stress in the Bushings	19
11	Barkhausen Signal Amplitude Versus Hoop Stress From Three NAS 537-12P-100 Bushings Stress Applied Using Clamping Fixture	21
12	Normalized Barkhausen Signal Amplitude Versus Hoop Stress From Three NAS 537-12P-100 Bushings Stress Applied Using Clamping Fixture	22
13	Barkhausen Signal Amplitude Versus Hoop Stress From Three NAS 537-12P-56 Bushings Stress Applied Using Clamping Fixture	23
14	Normalized Barkhausen Signal Amplitude Versus Hoop Stress From Three NAS 537-12P-56 Bushings Stress Applied Using Clamping Fixture	24
15	Barkhausen Signal Amplitude Versus Hoop Stress From Three NAS 537-8P-128 Bushings Stress Applied Using Clamping Fixture	25
16	Normalized Barkhausen Signal Amplitude Versus Hoop Stress From Three NAS 537-8P-128 Bushings Stress Applied Using Clamping Fixture	26

LIST OF ILLUSTRATIONS
(Cont'd)

<u>FIGURE</u>	<u>TITLE</u>	<u>PAGE</u>
17	Normalized Barkhausen Signal Amplitude Versus Hoop Stress From Three NAS 537-8P-37 Bushings Stress Applied Using Clamping Fixture	27
18	Barkhausen Signal Amplitude Versus Hoop Stress From Three NAS 537-8P-37 Bushings Stress Applied Using Clamping Fixture	28
19	Average Barkhausen Signal Amplitude Versus Stress for NAS 537-8P-128 Bushing Thermally Fitted Into 7075 Aluminum Cylinder	30
20	Average Barkhausen Signal Amplitude Versus Stress for NAS 537-12P-56 Bushing Thermally Fitted Into 7075 Aluminum Cylinder	31
21	Comparison of Major Stresses Produced in a Steel Bushing by a Thermal Interference Fit and Major Stresses Produced by the Clamping Fixture	32

LIST OF TABLES

<u>TABLE</u>	<u>TITLE</u>	<u>PAGE</u>
1	Results of Thermal Interference Fit Analysis	6
2	Drag Strut Bushing Specimens	9

I. INTRODUCTION

The assembly technique of differential thermal interference fits to secure steel bushings in aluminum parts as shown in Figure 1 is typical of many aircraft components. The drag strut is a forging of 7075 aluminum with NAS steel bushings assembled in it using differential thermal interference fits. The integrity of the assembly is totally dependent on the frictional forces produced at the steel aluminum interface by the dimensional interference between the aluminum part and the bushing. A nondestructive measurement of the stresses produced in the bushing is needed to verify the integrity of these thermal interference fits. This measurement would provide a means for determining that the desired stress level has been obtained in the assembly. Southwest Research Institute has pioneered the development of a nondestructive method for measuring stress based on Barkhausen noise analysis which may offer a practical solution to this problem. Thus, a program of Barkhausen noise acquisition and analysis was performed to determine the feasibility of using this measurement method to verify the integrity of interference fits.

5912

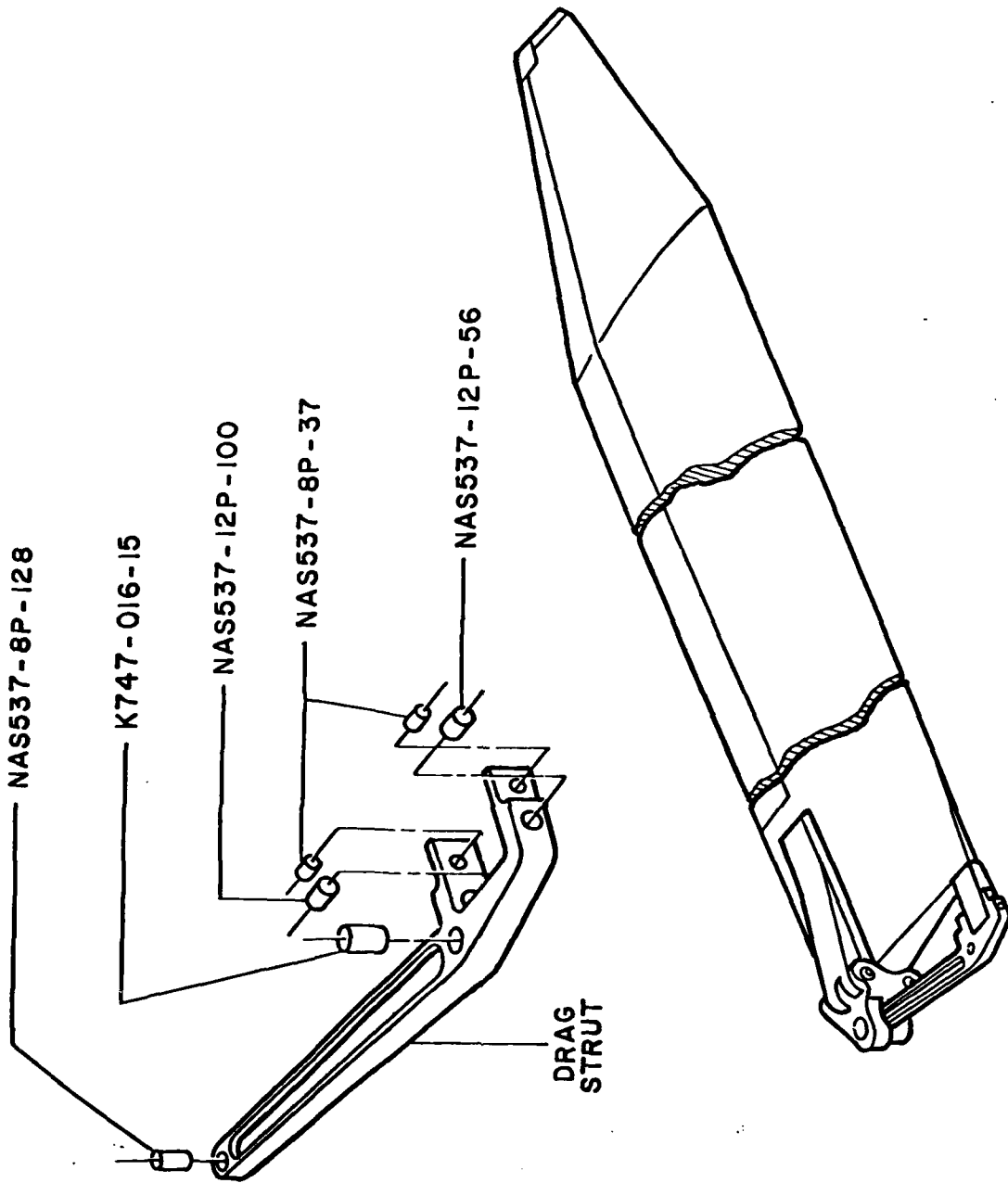


FIGURE 1. HELICOPTER DRAG STRUT ASSEMBLY

II. SUMMARY

Existing Barkhausen probes were adapted for acquiring Barkhausen data from bushings. Initially, data was acquired using a simple clamping fixture to produce hoop stresses in the bushing; tangential strain was measured by a strain gage attached to the bore of the bushing and Barkhausen data were obtained from the bore and also from the edge of the steel bushing.

The first task in this investigation was to prepare a mathematical analysis of the thermal fits as specified on KAMAN Aerospace Corporation Drawing No. K747-072 titled "Fitting Assembly, Drag Strut Rotor Blade." In this analysis, the range of dimensional interference between the bushing and the hole at ambient temperature and at the recommended assembly temperatures were calculated. Also, the values of hoop stress produced at ambient temperature in both the aluminum drag strut and in the steel bushing after assembly were calculated for each size of the bushing in the assembly. It was found that for several of the bushing sizes at the recommended assembly temperatures the outside diameter of the bushing was larger than the inside diameter of the hole into which they were to fit. This means that with a differential temperature of 400°F between the steel bushing and the aluminum drag strut, these bushings were a slight press fit into the holes. This type of press fit may cause material to be broached from the surface of the aluminum hole when the bushing is pressed into place.

The results of this investigation show that correlation between the Barkhausen measurements and the strain gage measurements of hoop stress in the bushing as produced by a simple clamping fixture was good. This clamping fixture produced a biaxial stress in the bushing composed of a compressive hoop stress and a compressive radial stress. The uses of the clamping fixture as a simulation of a thermal interference fit prove to be inadequate since it was determined that the thermal fit produced a third major stress in the axial direction in addition to the hoop and radial stresses. The results of experiments using actual thermal interference fit bushings into aluminum housing to correlate Barkhausen measurements with hoop stress as measured by a strain gage were encouraging, but inconsistent. This inconsistent behavior may be caused by the assembly process which was used or by the effects axial stress produced in the bushing.

Accordingly, it is recommended that a follow-on program, using a probe designed specifically for NAS bushings, be conducted with measurements being made on bushings inserted into actual drag struts. This investigation will help evaluate the process of utilizing the Barkhausen stress measurement system on production drag struts.

III. ANALYSIS OF DIFFERENTIAL THERMAL INTERFERENCE FITS

The analysis of the differential thermal interference fits is based on dimensions specified on Kaman Aerospace Corporation, drawing K747-072 titled "Fitting Assembly, Drag Strut Rotor Blade." The following values were calculated based on the dimensions and tolerances given on the assembly drawing:

1. The maximum and minimum clearance possible between the hole and the bushings at the recommended assembly temperatures of -200°F for the bushing and $+200^{\circ}\text{F}$ for the aluminum.
2. The maximum and minimum interference fits possible at ambient temperature of 75°F .
3. The maximum and minimum hoop stress possible in the NAS bushing.
4. The maximum and minimum hoop stress possible in the aluminum drag strut.

These values are given in Table I for the four NAS bushings used in this investigation.

Figure 2 is a graph of the interference fit vs. diameter of the bushing. The diagonal line is the point where the bushing will just slip into the hole in the drag strut at the recommended differential temperature of 400°F . The dots with the interconnecting bar show the tolerance range of interference for each of the NAS bushings as specified on the assembly drawing. All values above the diagonal line will be interference fits at the recommended assembly temperatures, while all values below the diagonal line will be slip fits at the recommended assembly temperatures. It should be noted that of the four different diameter bushings specified only one is a slip fit at the recommended assembly temperatures. The computer program utilized to calculate the hoop stresses for the thermal interference fits is presented in Appendix A.

TABLE I
RESULTS OF THERMAL INTERFERENCE FIT ANALYSIS

BUSHING TYPE	NAS537-8P	NAS537-12P	K747-016-15	K737-016-17
Nominal Bushing I.D./O.D.	0.484/0.626	0.734/0.940	0.875/1.1	0.406/0.696
* Clearance with Aluminum @ 200°F Bushings @ -200°F				
Minimum (inches)	-0.0000	-0.0002	+0.0003	0.0002
Maximum (inches)	-0.0013	-0.0017	+0.0023	-0.0008
* Clearance with Aluminum @ 75°F Bushings @ 75°F				
Minimum (inches)	-0.0025	-0.0037	-0.0020	-0.0022
Maximum (inches)	-0.0038	-0.0052	-0.0040	-0.0035
Hoop Stress in Aluminum @ 75°F				
Minimum (KSI)	16.5	19.8	9.8	18.6
Maximum (KSI)	25.0	27.9	19.5	29.7
Hoop Stress in Bushings @ 75°F				
Minimum (KSI)	72.9	61.9	25.5	44.3
Maximum (KSI)	111.0	88.9	50.9	75.5

* Clearance is positive number
Interference is negative number

5913

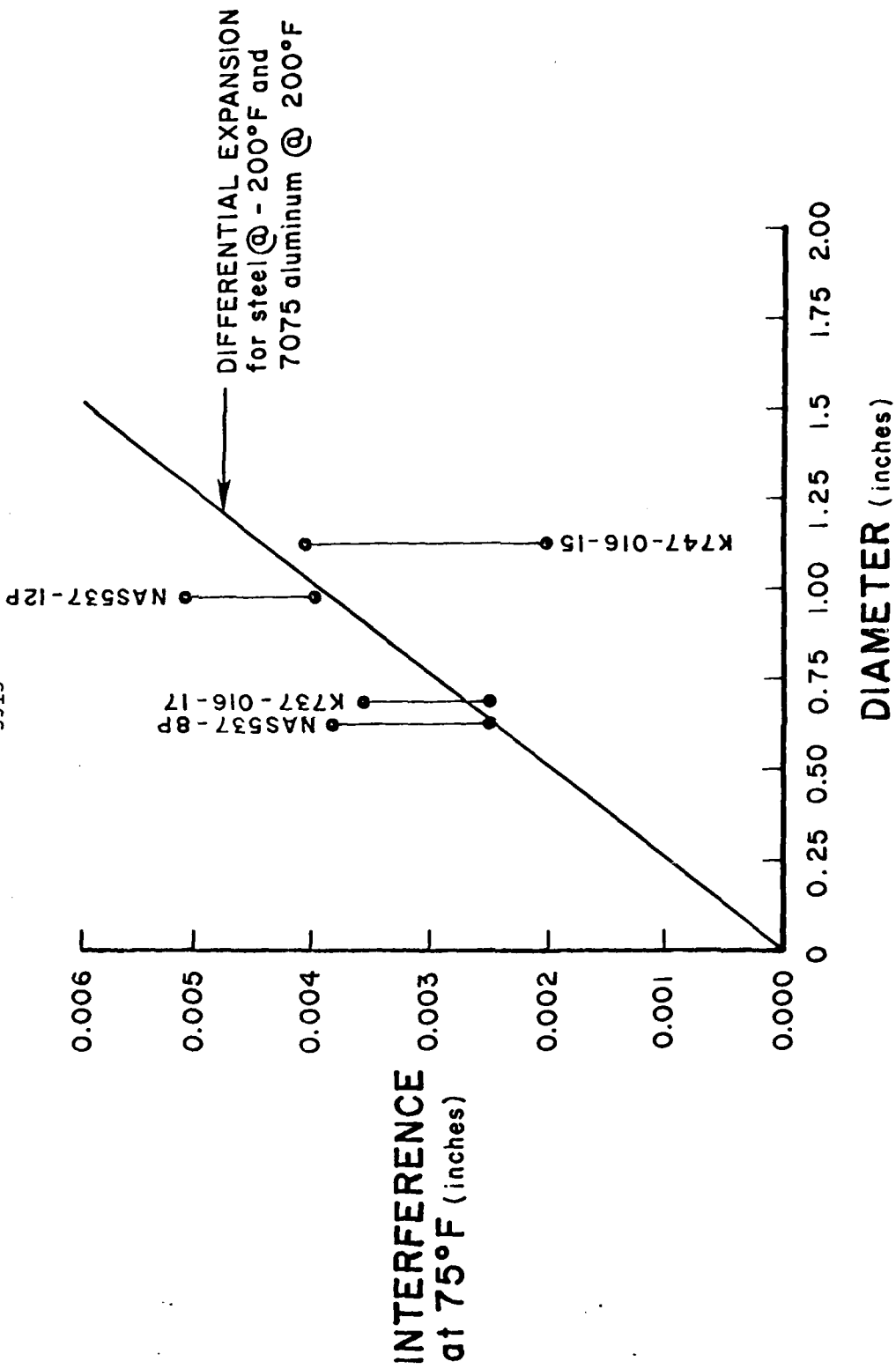


FIGURE 2. CALCULATED RANGE OF INTERFERENCE AT 400°F DIFFERENTIAL TEMPERATURE FOR EACH BUSING DIAMETER

IV. SPECIMENS AND TEST EQUIPMENT

Six different bushing types were selected for the investigation as shown in Table II. Orders were placed for ten bushings of each type. All four of the NAS 537 bushings were quickly procured, but the K747-016-15 and the K737-016-17 bushings could not be delivered in such small quantities. Accordingly, a request was made to the Army to provide these specimens. Army personnel found that these bushings were in short supply and it was agreed that these two bushing types would not be included in the investigation.

For the purpose of this investigation, each bushing specimen was marked with an identification number. The identification numbering system is shown as follows:

10 ea.	NAS 537-12P-100	I.D. No. 1 through 10
10 ea.	NAS 537-12P-56	I.D. No. 11 through 20
10 ea.	NAS 537-8P-128	I.D. No. 21 through 30
10 ea.	NAS 537-8P-37	I.D. No. 31 through 40

To simulate the drag strut holes into which the steel bushing are assembled, 7075-T6 aluminum bar stock, two inches in diameter was machined to the length and hole diameter specified on drawing K747-072. Figure 3 shows the simple clamping fixture used to produce hoop stress in the bushings, while Figure 4 shows a typical bushing and the aluminum specimen in which the bushing was to be assembled.

The equipment used for this investigation was a "200 Series Barkhausen Stress Measurement System," produced by Southwest Research Institute. Two different Barkhausen probes were used, one was a general-purpose hand-held probe designed for flat surfaces and was used to acquire data from the end of the bushing, while the second probe was a special design which allowed data to be acquired from the bore of the bushing. This equipment is shown in Figure 5. A strain gage bridge for monitoring the strain gages mounted on the bore of the bushings was also used for this investigation.

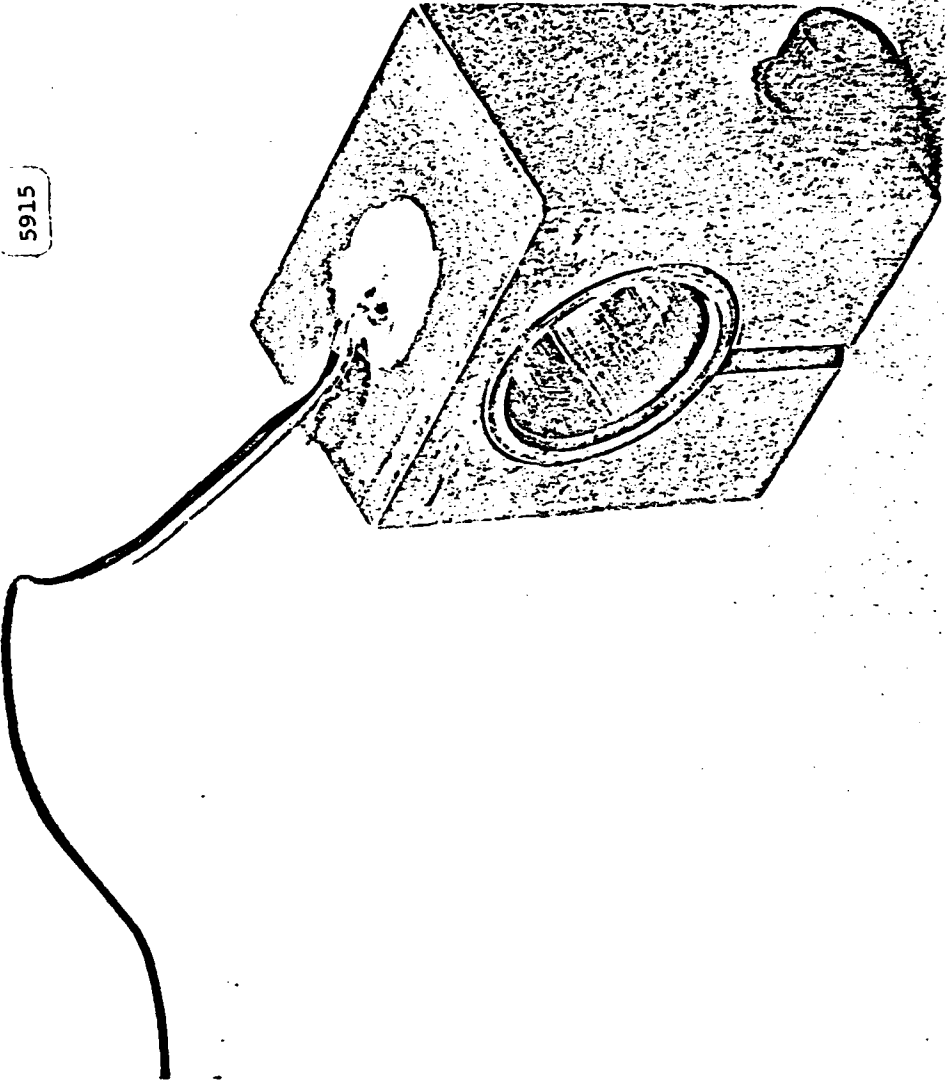
TABLE II

DRAG STRUT BUSHING SPECIMENS

Bushing Number	Nominal I.D. (in.)	Nominal O.D. (in.)	Nominal Length (in.)	Material
NAS537-8P-128	0.484	0.626	1.280	4130 Steel
NAS537-8P-37	0.484	0.626	0.370	4130 Steel
NAS537-12P-100	0.734	0.940	1.000	4130 Steel
NAS537-12P-56	0.734	0.940	0.560	4130 Steel
*K747-016-15	0.875	1.127	1.900	4340 Steel
*K737-016-17	0.406	0.696	1.260	4340 Steel

Finish: Cadmium Plate

* These bushings were not used in this investigation due to unavailability from stock.



5915

FIGURE 3. SIMPLE FIXTURE FOR APPLYING STRESS TO BUSHINGS

5914

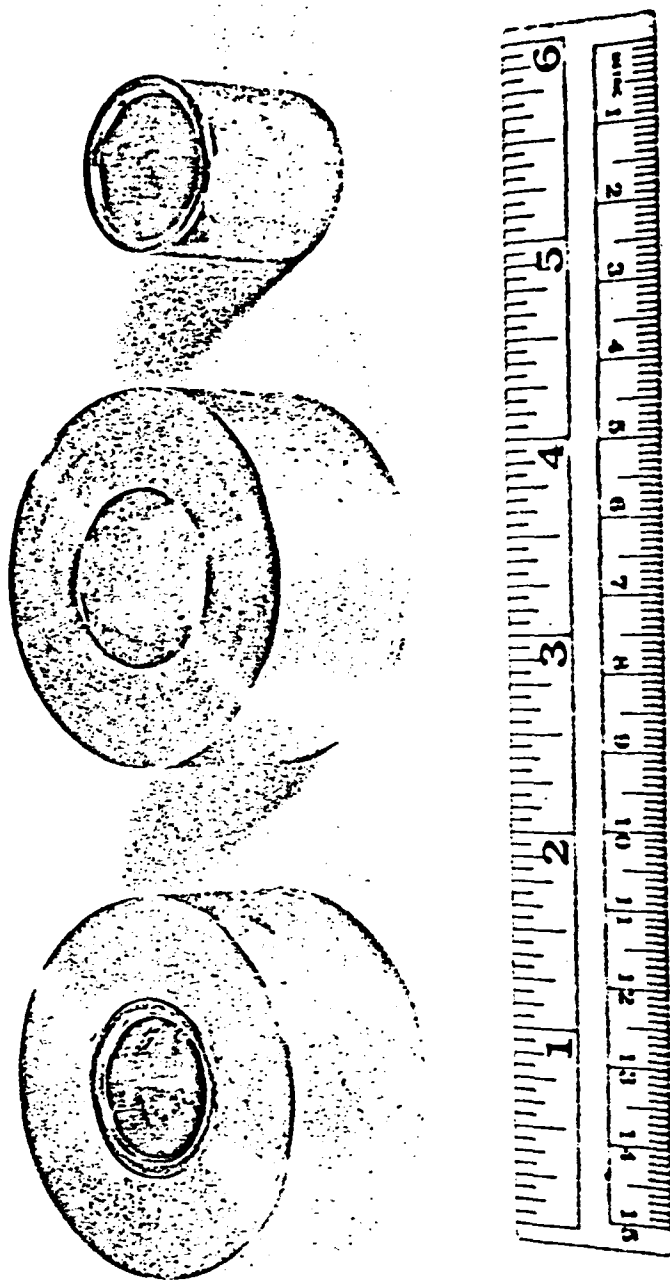


FIGURE 4. ALUMINUM TEST SPECIMEN AND BUSHING BEFORE AND AFTER ASSEMBLY

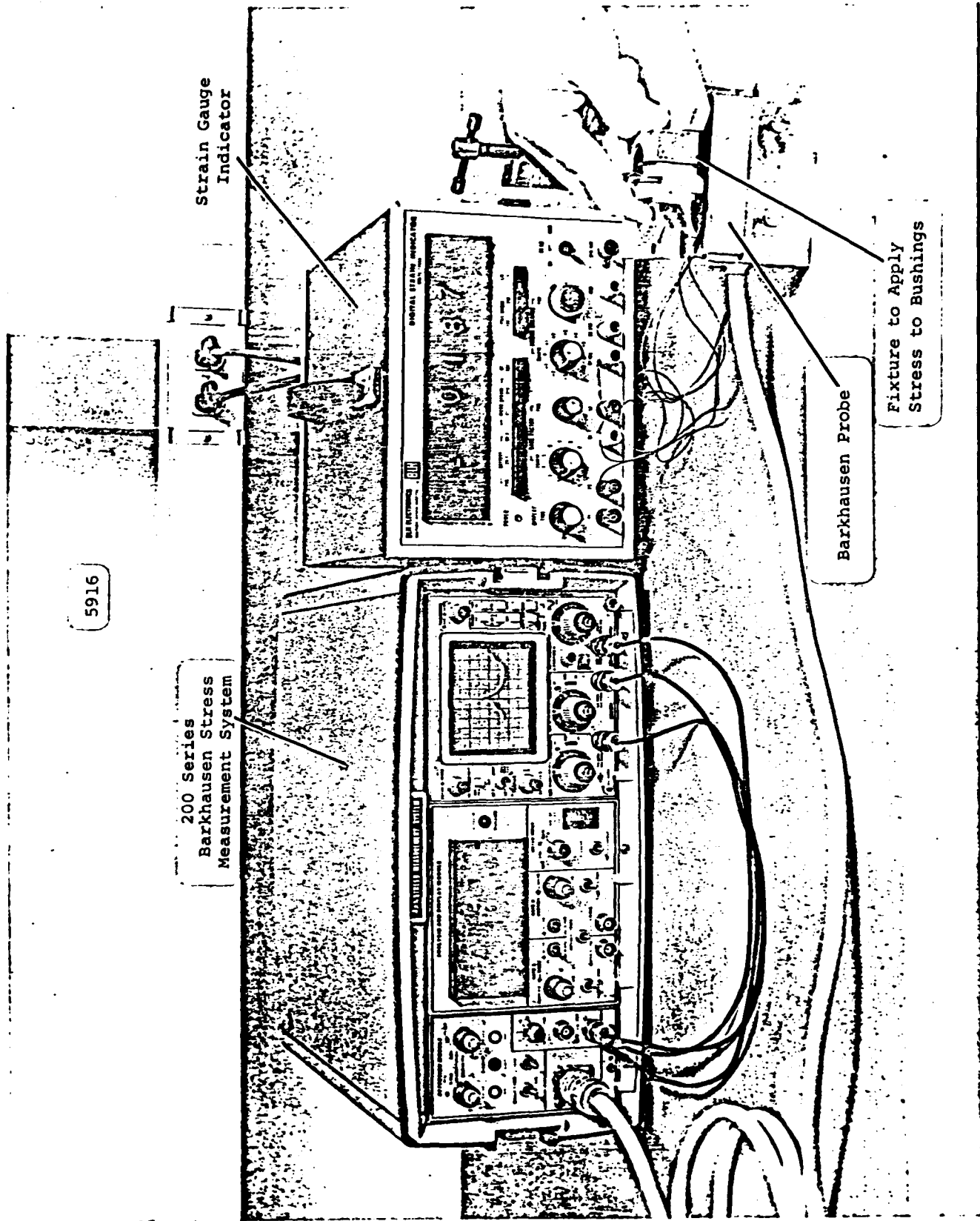


FIGURE 5. EQUIPMENT USED IN THIS INVESTIGATION

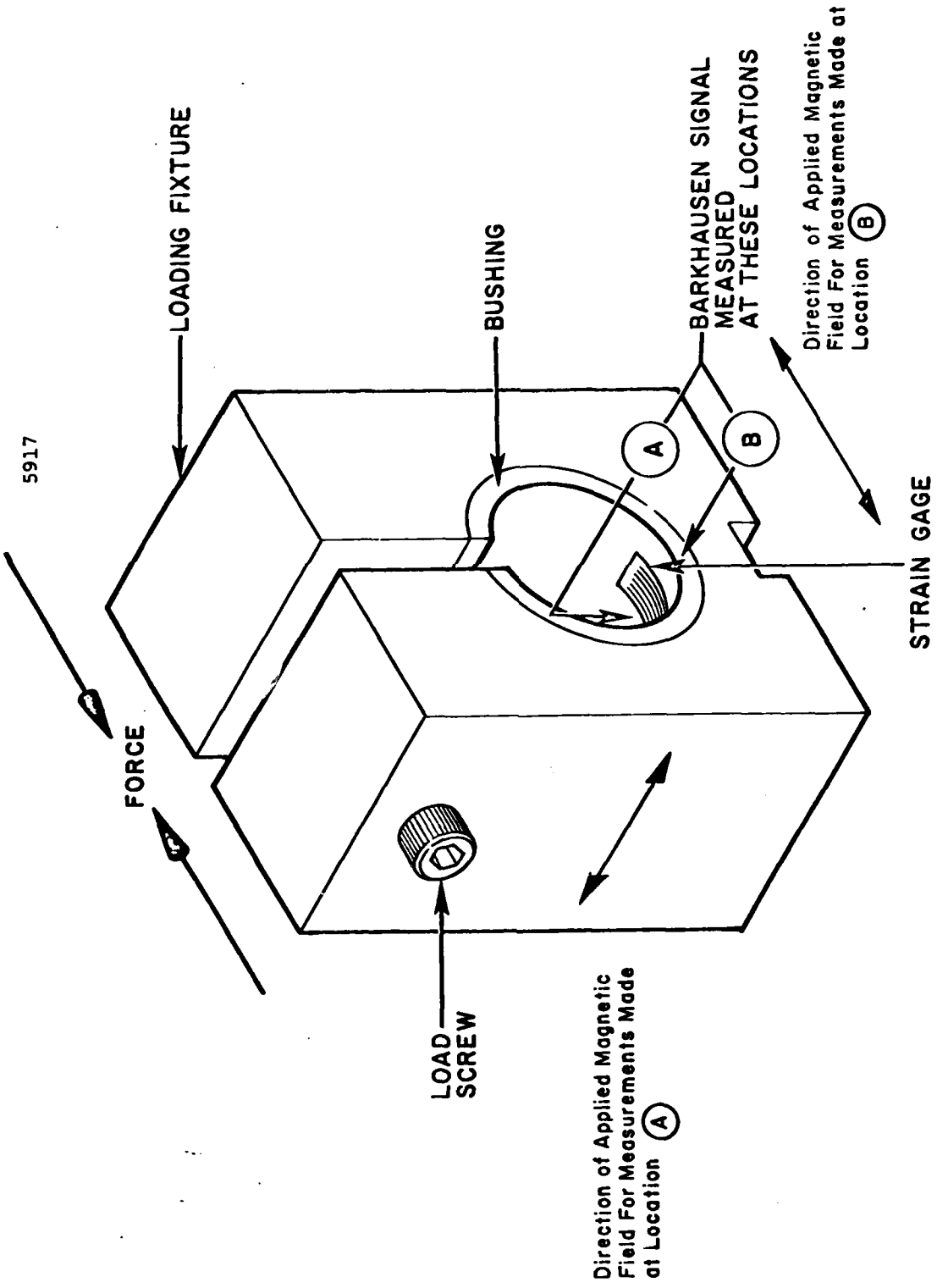
V. EXPERIMENTS

The first experiment performed on this investigation was designed to measure the Barkhausen signal amplitude versus strain gage response from a bushing, which had a small segment of material removed, with the stress applied by a simple loading fixture as shown in Figure 6. In this experiment, Barkhausen data were taken from two different locations (A and B) on the bushing in an effort to determine which was the optimum location for detecting the applied hoop stress.

A strain gage was mounted on the bore of the bushing 180° from the removed segment. Location "A" was approximately centered in the length of the bushing and was adjacent to the strain gage. Location "B" was on the edge of the bushing approximately 180° from the removed segment. Measurements at location "A" were made with the sensitive axis of the Barkhausen probe oriented along the axis of the bushing. Measurements at location "B" were made with the sensitive axis of the probe oriented in the tangential direction.

Figure 7 is a plot of measured Barkhausen signal amplitude at location "A" as measured at increasing values of applied compressive tangential stress on the inside bore of the bushing. The applied tangential stress values were calculated from the strain gage measurements. The cross-hatched area indicates the minimum and maximum tangential stress possible as determined by the mathematical analysis. Note that when the compression stress is below the minimum value a high Barkhausen signal amplitude is obtained and when the stress is above the maximum value, a smaller Barkhausen signal amplitude is obtained.

Figure 8 is a similar plot for location "B" on the edge of the bushing (strain was still measured on bore). For this location, compressive tangential stresses below the recommended minimum value result in low Barkhausen signal amplitudes and those above the maximum tangential stress result in higher Barkhausen amplitudes. Based on the results of this experiment, it was determined that both locations gave acceptable response to applied hoop stress, but location "B" showed greater sensitivity and better linearity through the entire range of applied stress. Also it should be noted that the simple probe design required



5917

FIGURE 6. LOADING FIXTURE SHOWING MEASUREMENT LOCATIONS ON A SPLIT BUSHING

5918

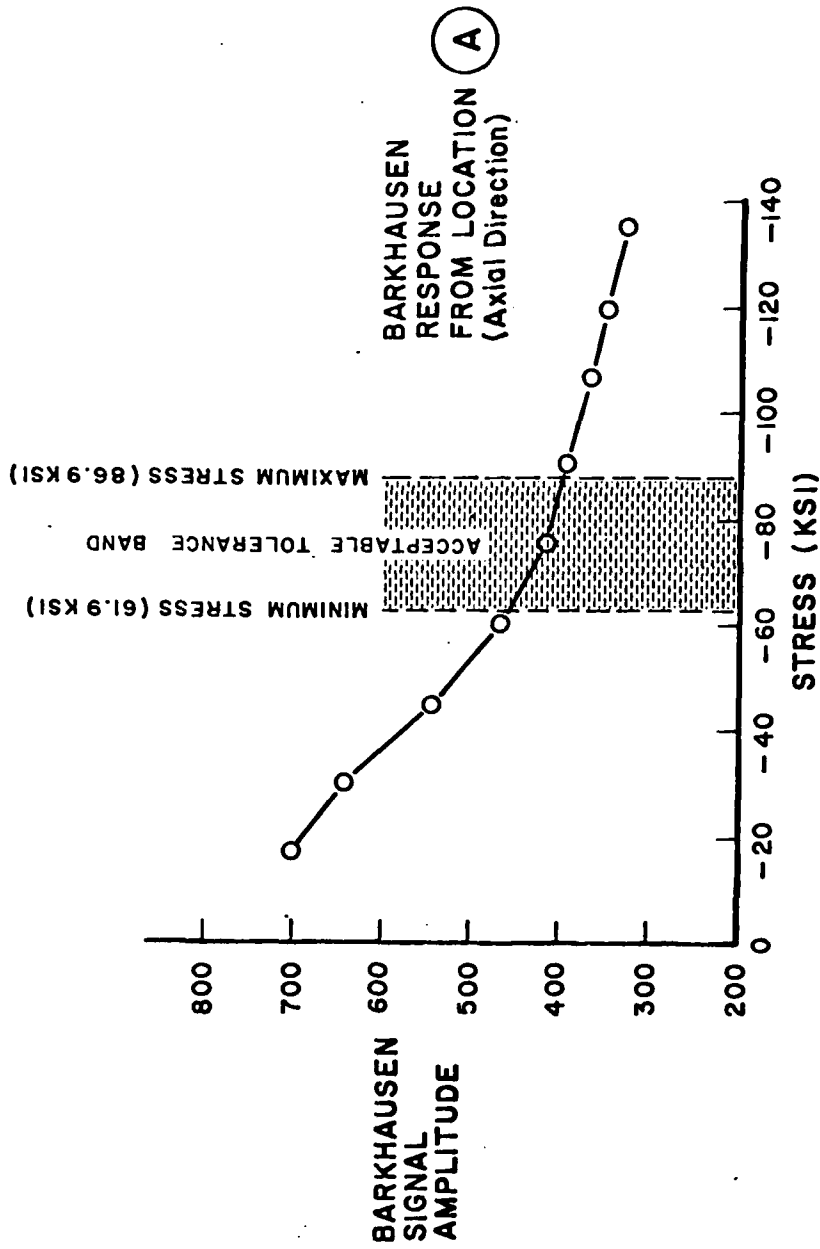


FIGURE 7. BARKHAUSEN SIGNAL AMPLITUDE VERSUS APPLIED HOOP STRESS AT LOCATION "A"

5919

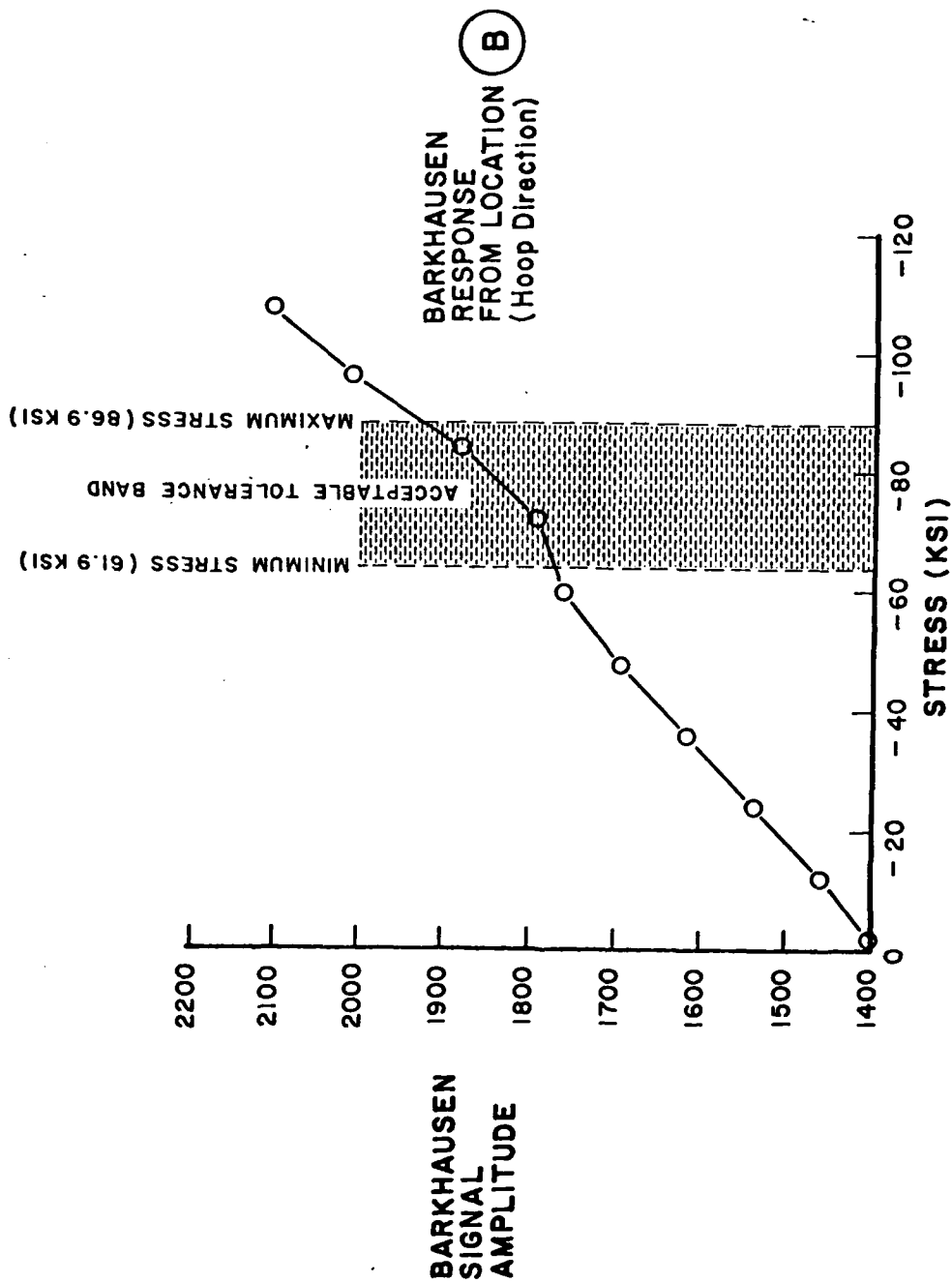


FIGURE 8. BARKHAUSEN SIGNAL AMPLITUDE VERSUS APPLIED HOOP STRESS AT LOCATION "B"

to make the Barkhausen measurement at the edge of the bushing as opposed to the center of the bore makes location "B" more attractive. Based upon these results, it was determined that for the bulk of the data in this investigation the Barkhausen measurements would be taken at the edge of the bushing as in location "B".

The next experiment was designed to determine the best magnetizing rate at which to obtain the Barkhausen measurements. Figure 9 shows two sets of curves taken at location "B" on the edge of the bushing. The two separate plots are for different magnetizing rates; the lower sets of data are for 0.5 Hz magnetizing rate and the upper sets of data are for 1.0 Hz magnetizing rate. For the lower sets, note that the triangular symbols (data set 1) are used for closed loop calibration starting near zero, increasing to 90 ksi stress and then decreasing to zero stress. In the same grouping of points, the + symbol (data set 2) also starts at zero stress and increases to 90 ksi stress and then decreases back to zero. A similar explanation applies to the open squares (data set 3) and diamond (data set 4), respectively. Note that the repeatability of the data are excellent and that the higher frequency of 1.0 Hz results in significantly higher Barkhausen value for zero stress and has a somewhat steeper slope. Based upon the results and our past experience with Barkhausen it was agreed that there was no advantage in using the higher magnetizing frequency of 1.0 Hz and a value of 0.5 Hz was selected to be used for the bulk of the experiments.

The following experiment was designed to evaluate the range of variation in Barkhausen readings obtained at no-load on the edge of the bushings in the no-load condition. Specimens 2 through 8 of NAS 537-12P-100 bushing were selected for this investigation and four readings were made on each bushing at 0, 90, 180 and 270°. Figure 10 shows that Barkhausen signal amplitudes have significant variation from one location to another on the same bushing and even a greater variation from one bushing to another. It is concluded that this variation is caused by a significant amount of residual stress variation in the edge of the bushings. Since the stress generated by the thermal interference fit will be superimposed upon the residual stress, the Barkhausen measurements

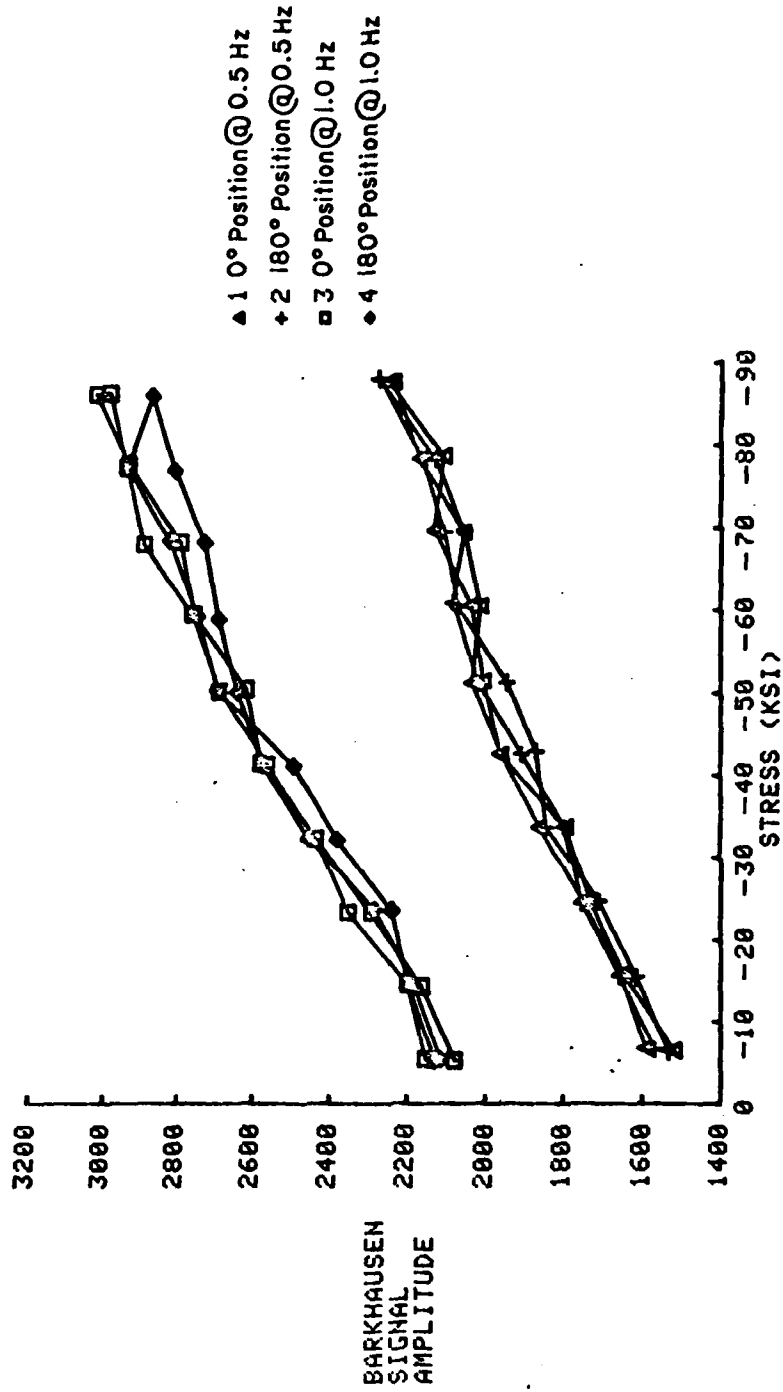


FIGURE 9. BARKHAUSEN SIGNAL AMPLITUDE VERSUS APPLIED HOOP STRESS AT 0.5 Hz AND 1.0 Hz MAGNETIZATION FREQUENCY

5921

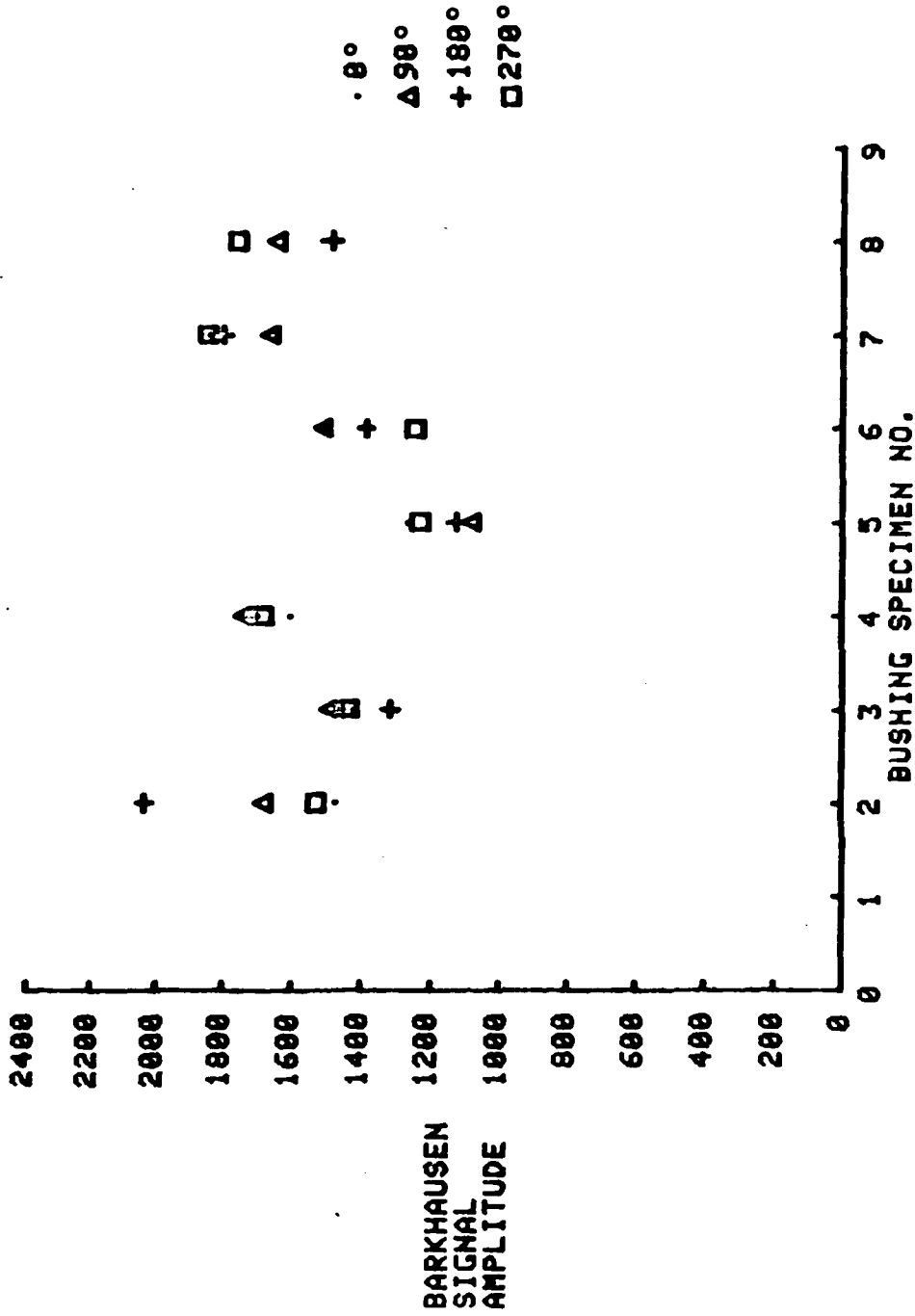


FIGURE 10. BARKHAUSEN SIGNAL AMPLITUDE VERSUS SPECIMEN NUMBER SHOWING AMPLITUDE VARIATIONS CAUSED BY RESIDUAL STRESS IN THE BUSHINGS

will indicate the algebraic sum of these stresses.

In the next section of this investigation, several specimens from each of the four NAS 537 bushing types were inserted into the loading fixture shown in Figure 4. Barkhausen signal amplitude data were obtained at two angular locations on the edge of each bushing, as the compressive hoop stress was increased from 0 to the maximum stress level which could be obtained using the simple clamping fixture. It should be noted that the maximum hoop stress values indicated in this experiment are a limitation of the loading fixture and not of the instrumentation. Figures 11 through 18 show the results of this experiment. Studying the results, it is noted that for a particular bushing type, each of the curves are similar in shape but may be displaced vertically on the Barkhausen signal amplitude axis. This displacement is caused by residual stress which exists in the part before the load is applied as indicated in the previous experiment, since the total stress is the sum of the residual and applied stresses. If the data are normalized by subtracting out the zero values, variation of the data are significantly reduced. Figure 11 shows the results from three specimens from the NAS 537-12P-100 group, while Figure 12 shows the same data which has been normalized. Likewise, the results and the normalized data are shown for the remaining bushing types in Figures 13 through 18. For these figures, the numbers following the data symbols are the bushing specimen number and the angular location with respect to the strain gage.

The results from these data show that with the exception of offset caused by residual stress in the specimen, the calibration curves for each of the specimens within a bushing type, are approximately the same. It is believed that for each bushing type a single calibration curve with a correction factor to account for the variation in residual stress would allow accurate measurements of the hoop stress in the bushing after it has been assembled in an aluminum housing.

Based on the positive results shown in the previous portions of this program one bushing of each specimen type was assembled, per instructions on KAMAN assembly drawing, into aluminum specimens 2.0 in. O.D. After each

5922

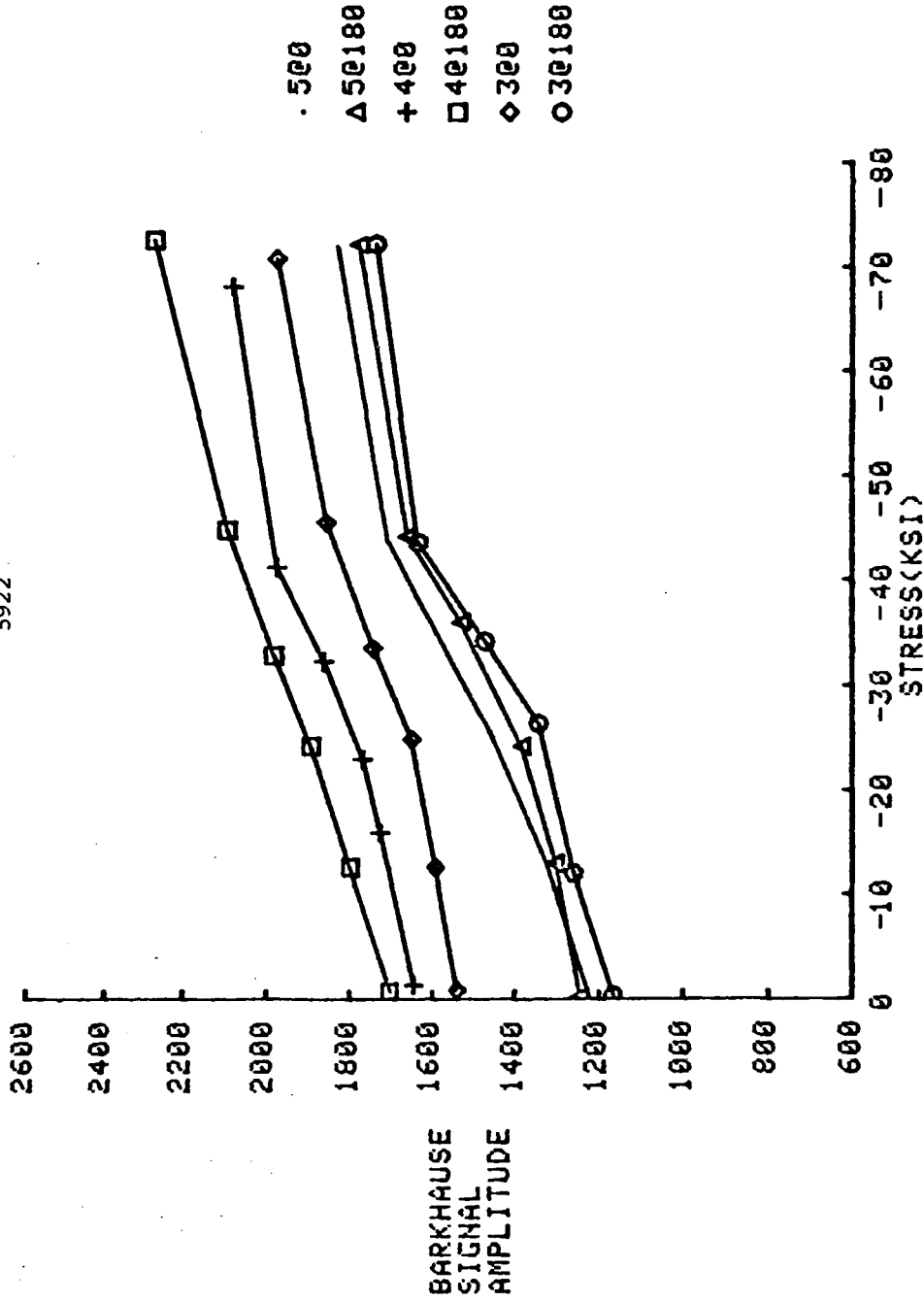


FIGURE 11. BARKHAUSEN SIGNAL AMPLITUDE VERSUS HOOP STRESS FROM THREE NAS 537-12P-100 BUSHINGS STRESS APPLIED USING CLAMPING FIXTURE

5923

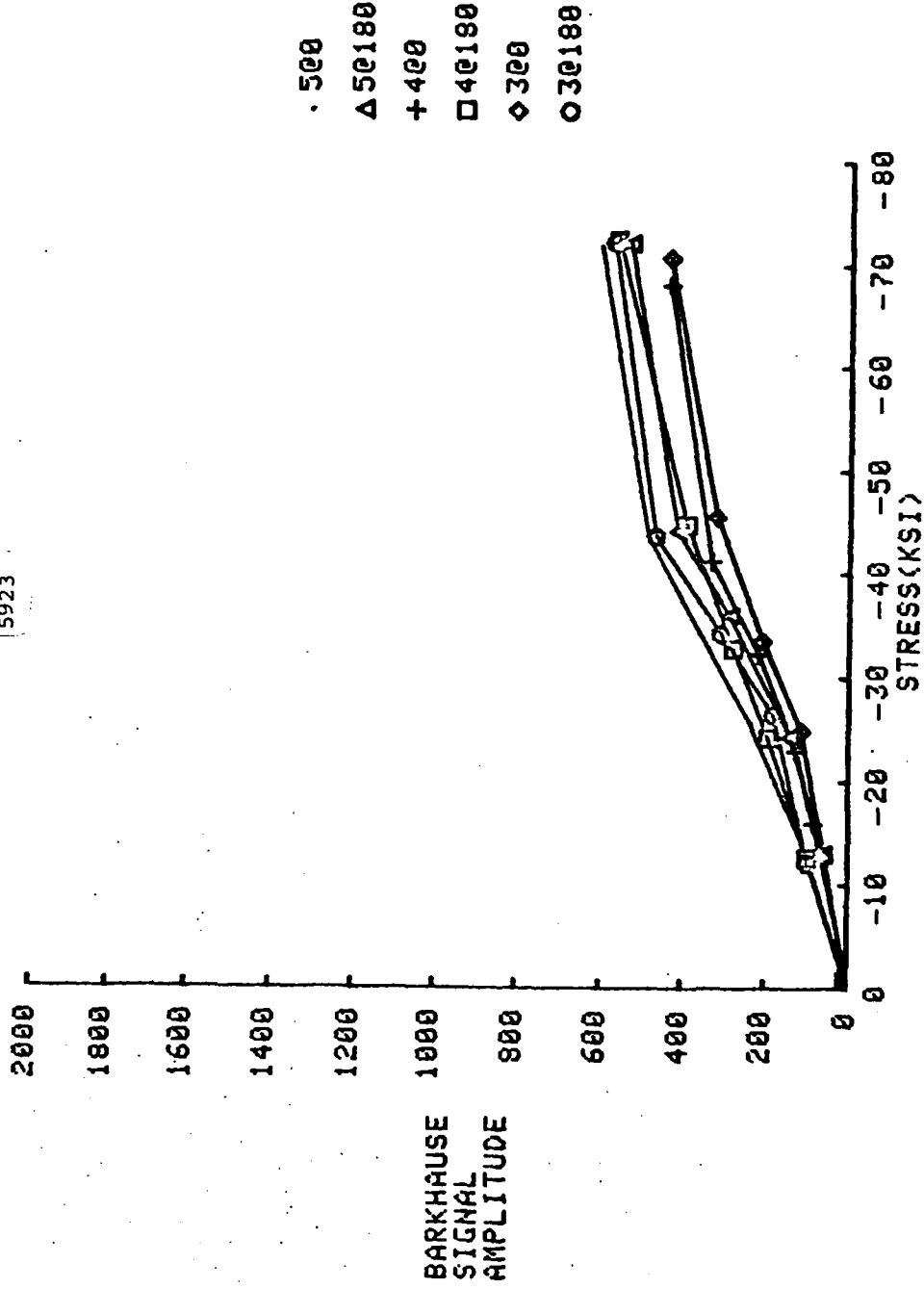


FIGURE 12. NORMALIZED BARKHAUSEN SIGNAL AMPLITUDE VERSUS HOOP STRESS FROM THREE NAS 537-12P-100 BUSHINGS STRESS APPLIED USING CLAMPING FIXTURE

5924

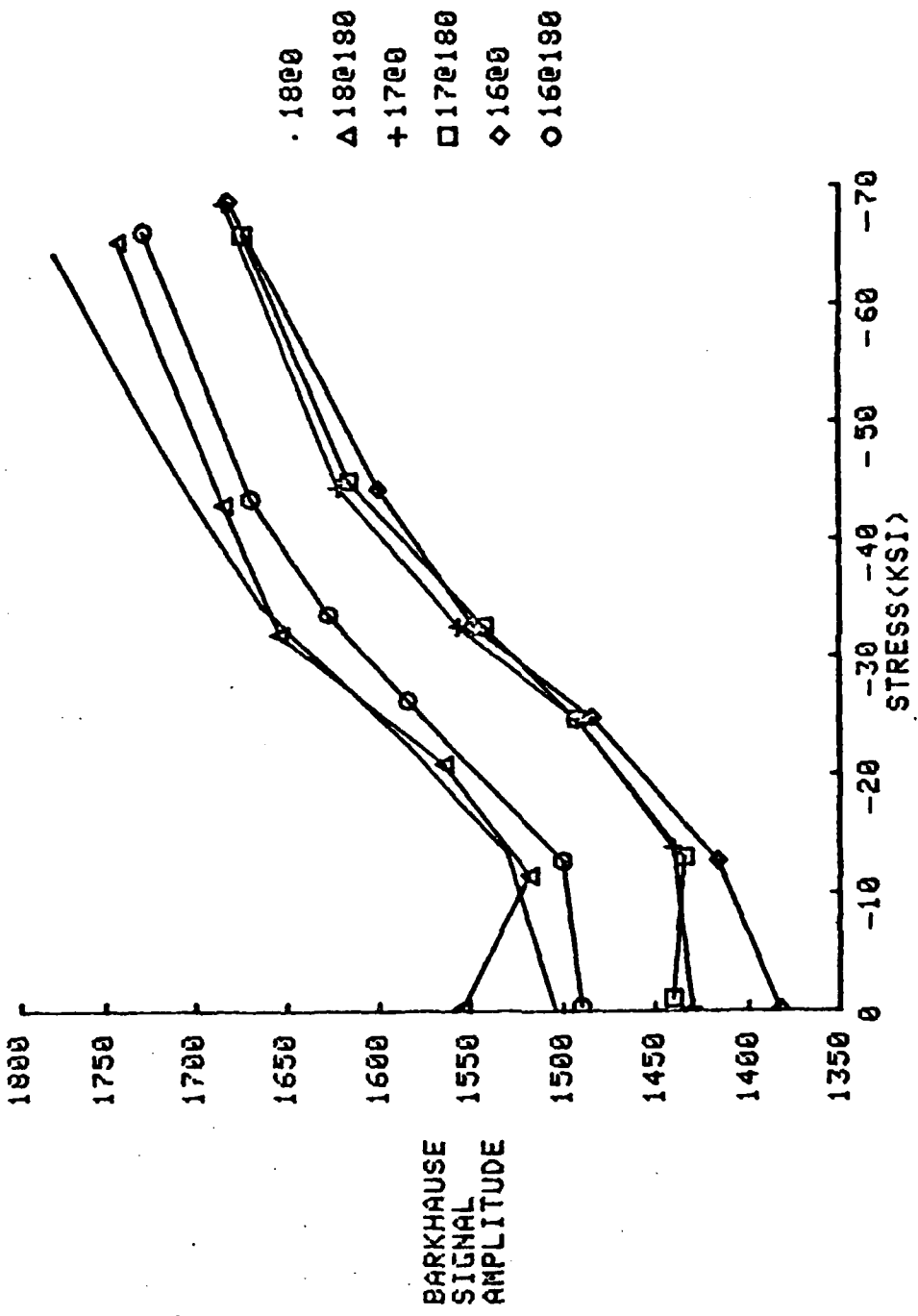


FIGURE 13. BARKHAUSEN SIGNAL AMPLITUDE VERSUS HOOP STRESS FROM THREE NAS 537-12P-56 BUSHINGS STRESS APPLIED USING CLAMPING FIXTURE

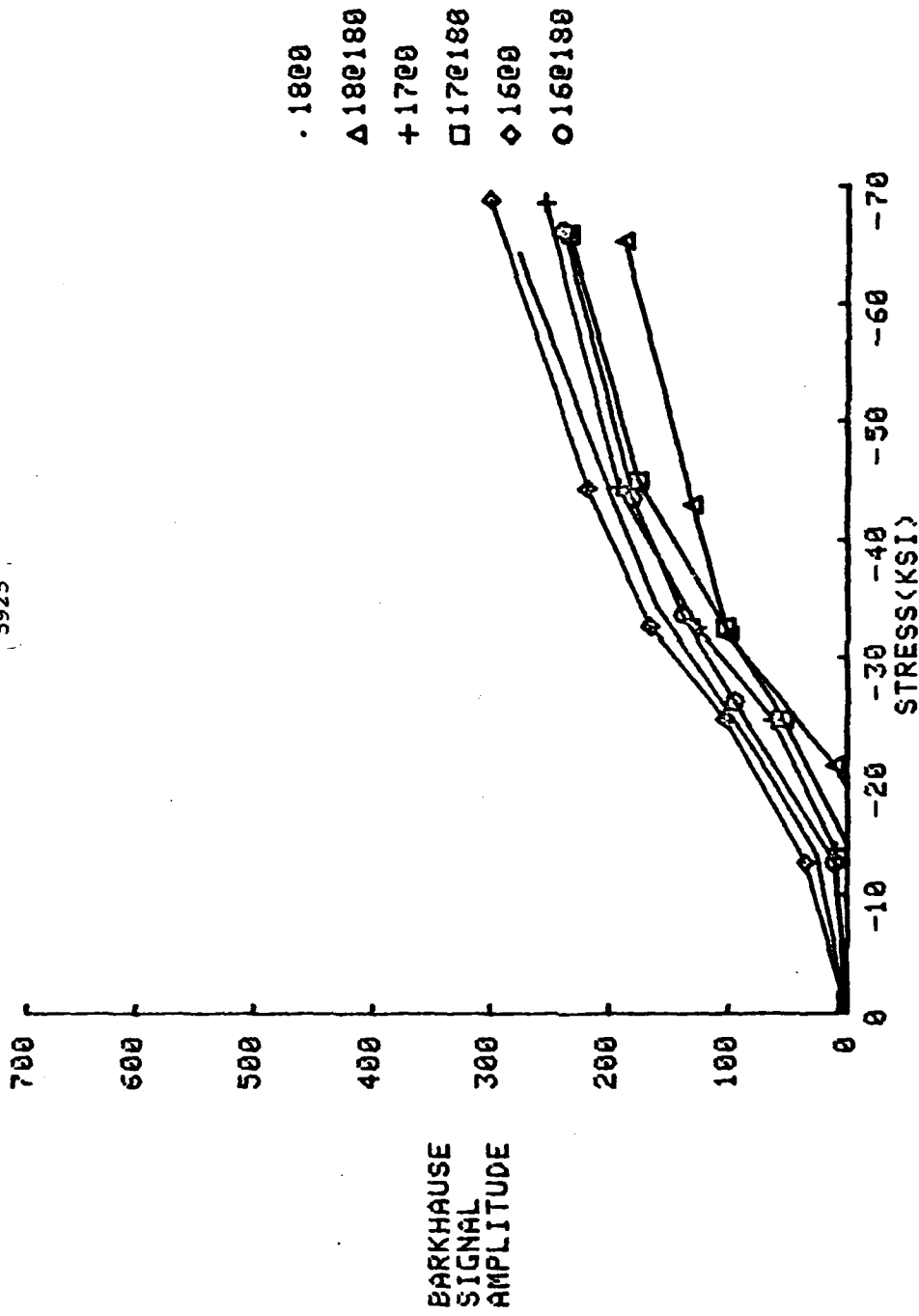


FIGURE 14. NORMALIZED BARKHAUSEN SIGNAL AMPLITUDE VERSUS HOOP STRESS FROM THREE NAS 537-12P-56 BUSHINGS STRESS APPLIED USING CLAMPING FIXTURE

5926

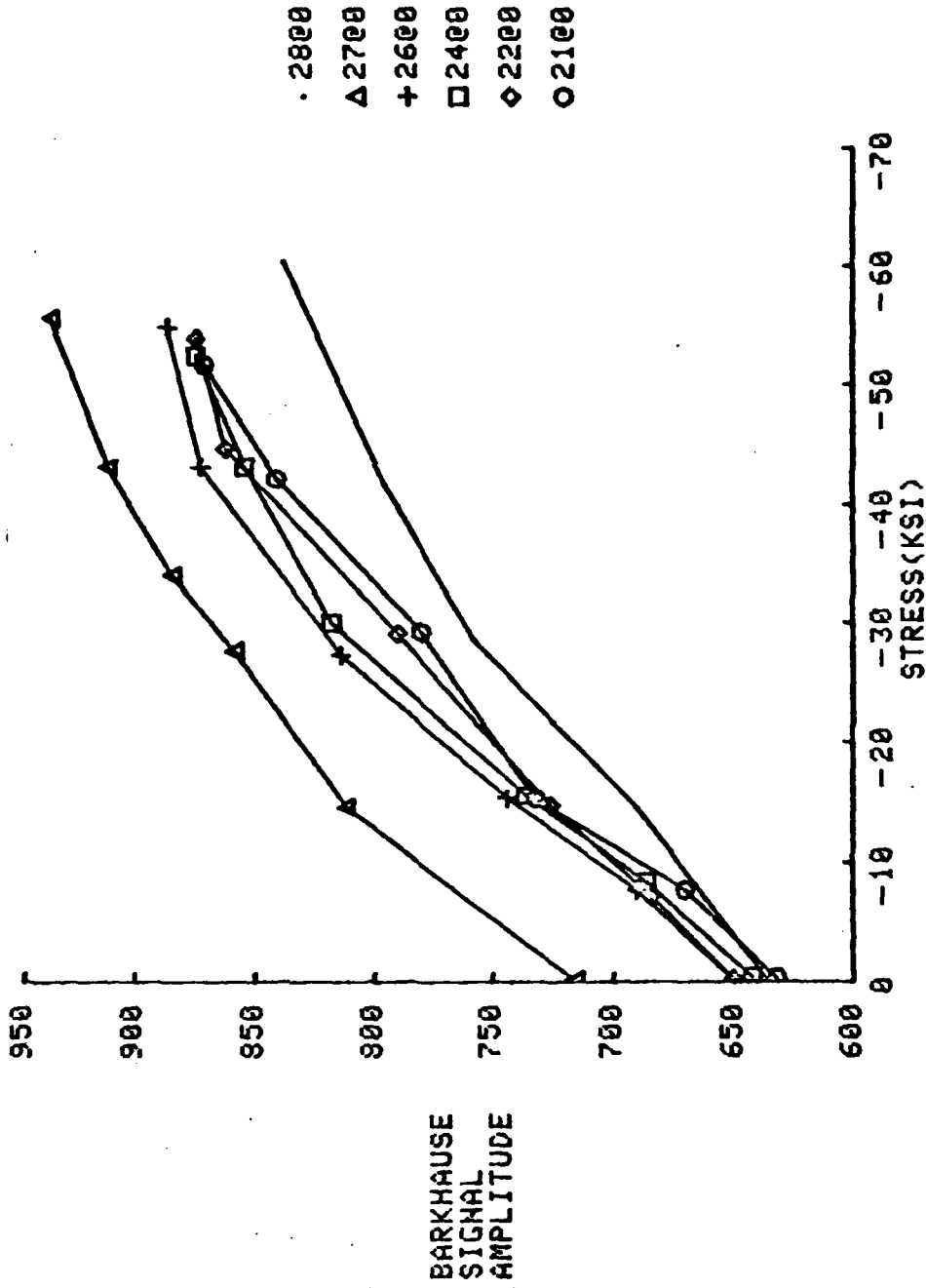


FIGURE 15. BARKHAUSEN SIGNAL AMPLITUDE VERSUS HOOP STRESS FROM THREE NAS 537-8P-128 BUSHINGS STRESS APPLIED USING CLAMPING FIXTURE

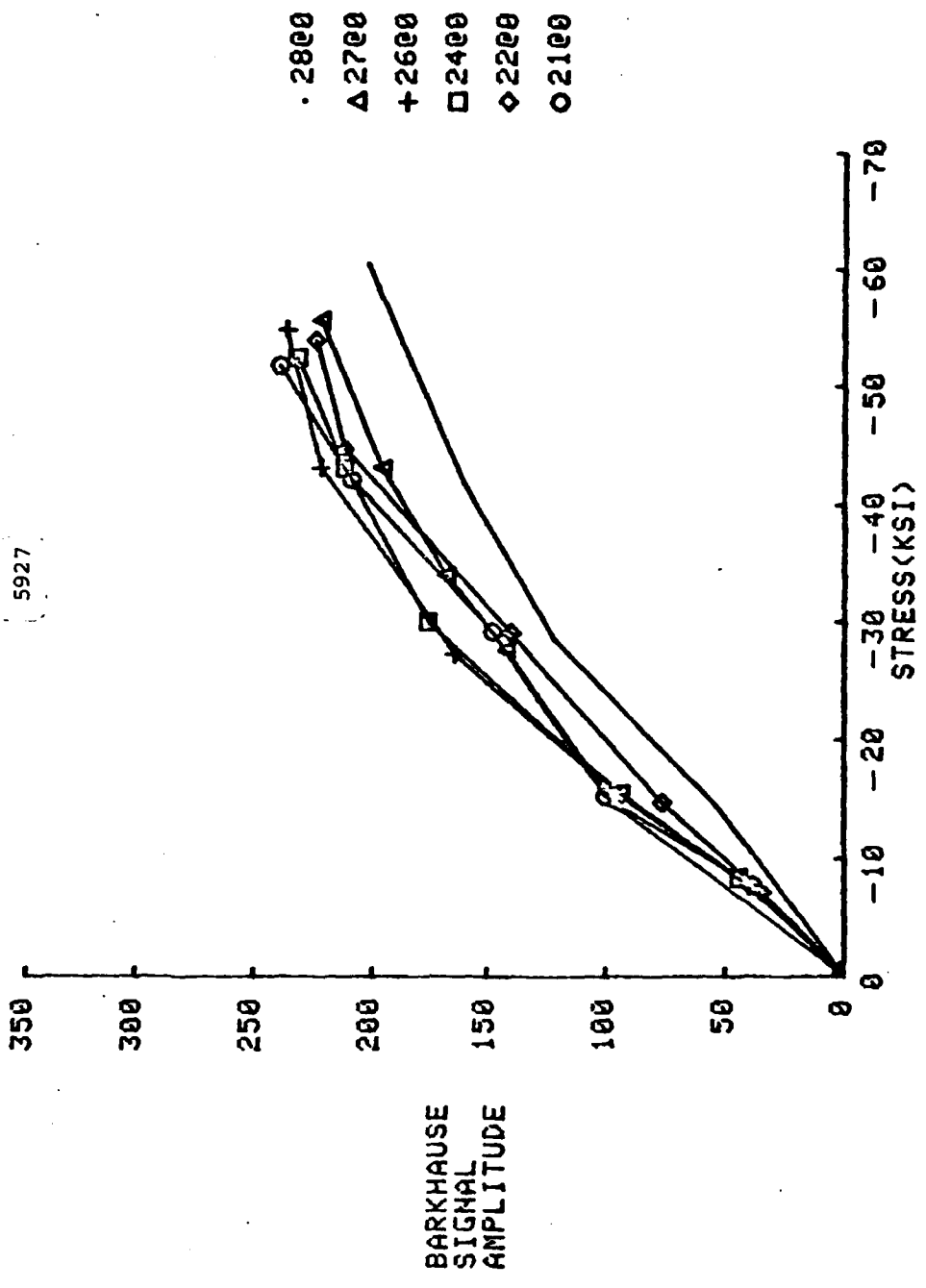


FIGURE 16. NORMALIZED BARKHAUSEN SIGNAL AMPLITUDE VERSUS HOOP STRESS FROM THREE NAS 537-8P-128 BUSHINGS STRESS APPLIED USING CLAMPING FIXTURE

(5928)

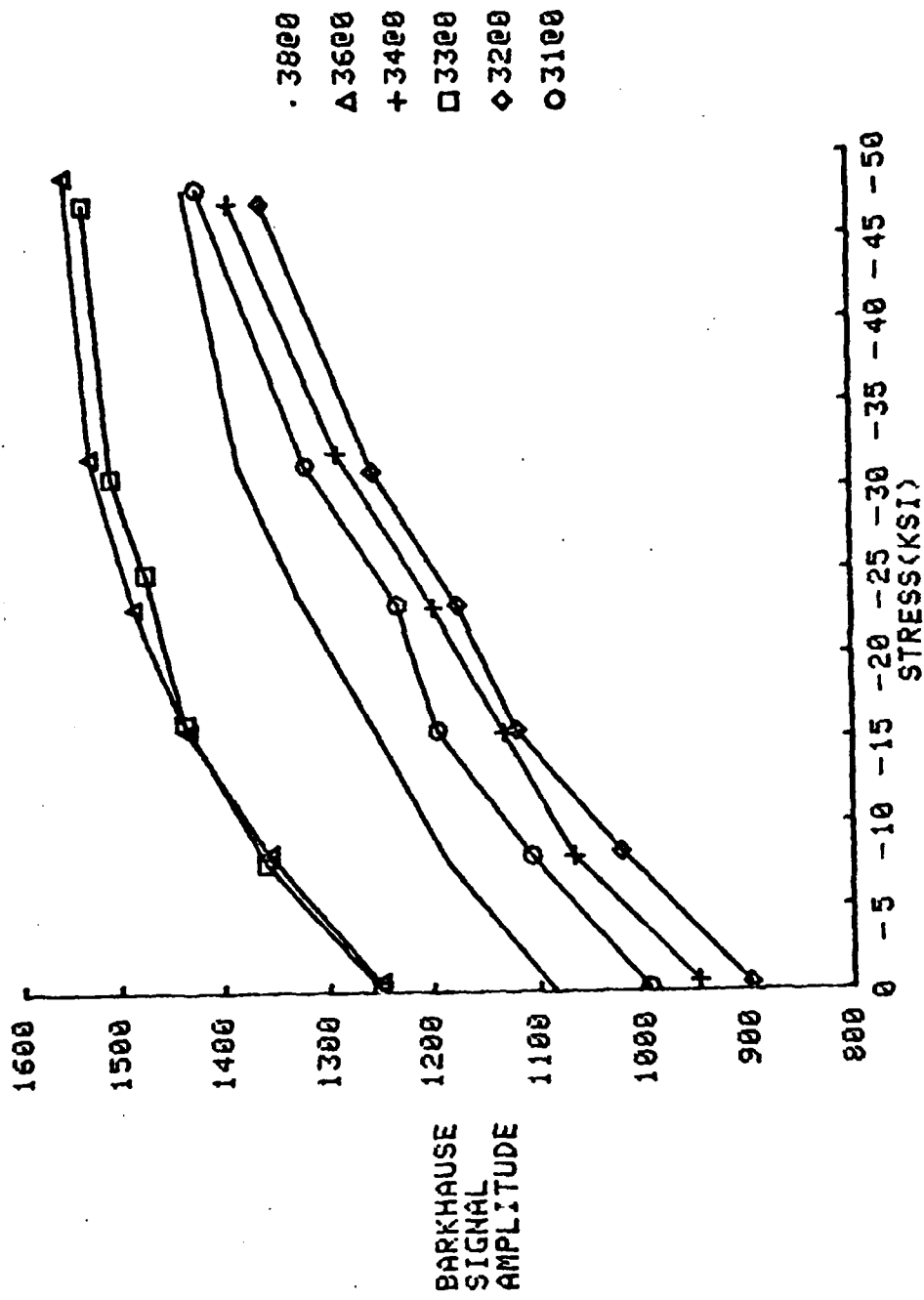


FIGURE 17. NORMALIZED BARKHAUSEN SIGNAL AMPLITUDE VERSUS HOOP STRESS FROM THREE NAS 537-8P-37 BUSHINGS STRESS APPLIED USING CLAMPING FIXTURE

5929

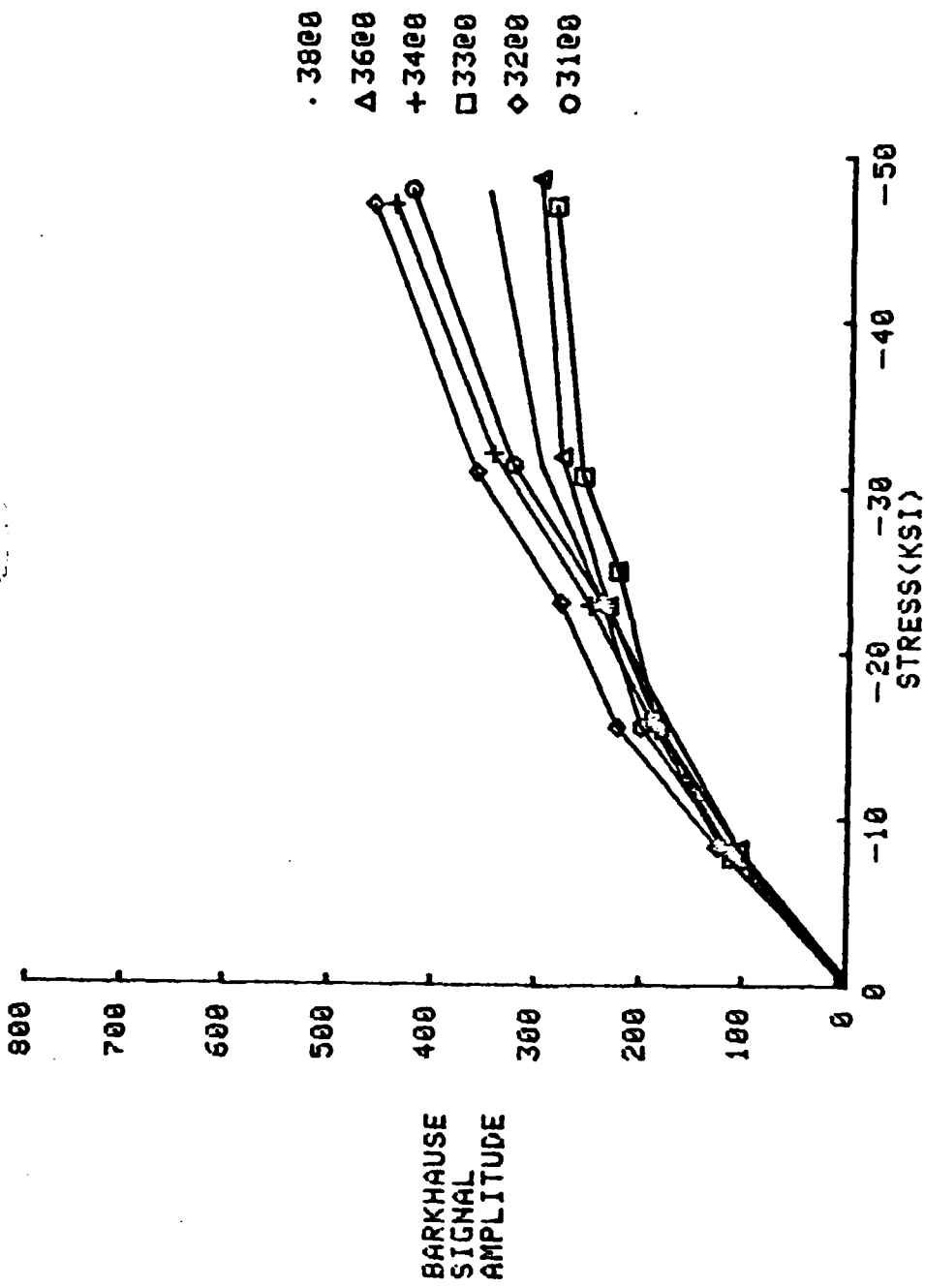


FIGURE 18. BARKHAUSEN SIGNAL AMPLITUDE VERSUS HOOP STRESS FROM THREE NAS 537-8P-37 BUSHINGS STRESS APPLIED USING CLAMPING FIXTURE

of the specimens was thermally fitted into its aluminum housing, a strain gage was mounted on the inside bore of each bushing. The procedure was to first measure the Barkhausen signal amplitude at the edge of the bushing at several locations and measure the hoop strain in the bushing as indicated by the strain gage on the bore of the bushing. Next material was removed from the outside of the aluminum cylinder which causes a reduction in the compressive hoop stress level in the bushing. A calibration of the aluminum outside housing diameter versus predicted stress in the bushing was calculated for interference fits of .0035 in. and .0050 in. Based upon the results of this calculation, it was decided that after each set of measurements, 50% of the remaining wall thickness of the aluminum cylinder would be removed. Each time after removing material from the outside wall of the aluminum cylinder, new Barkhausen measurements and strain indications were recorded.

Figures 19 and 20 show typical results of this experiment. These figures show the average Barkhausen amplitude versus hoop stress. The average Barkhausen signal consists of data measured at four locations 90° apart on the edge of the bushing. These results show essentially the same overall sensitivity as shown in the results using the clamping fixture to apply the load, but the data did not always follow the calibration curve obtained by using the clamping fixture over the total load range. Since the results were not as expected, two more specimens were prepared and the experiment carefully repeated. The result was essentially the same.

A careful analysis of the differences in stresses produced in the bushing by the clamping fixture and the stresses produced by the thermal fit was made. Figure 21 illustrates the differences. The clamping fixture produces compressive hoop stress, compressive radial stress and essentially no axial stress, while the thermal fit produces compressive hoop, compressive radial and compressive axial stress as because of the differential shrinkage. Thus, there is a difference in the axial stress produced, which for the fixture is essentially zero, while for thermal fits the axial stress is not zero and may be variable depending on the frictional forces at the steel-aluminum interface.

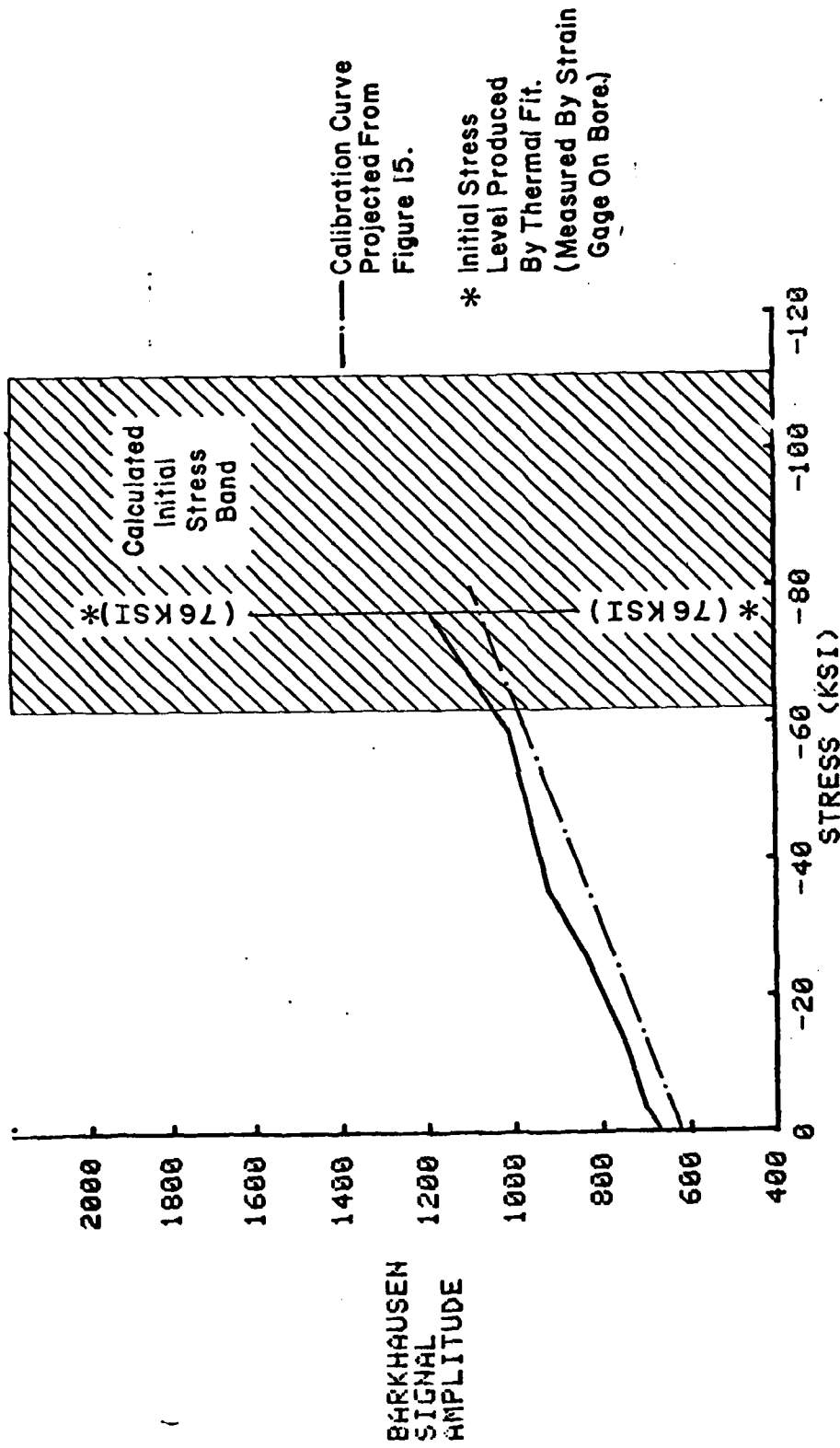


FIGURE 19. AVERAGE BARKHAUSEN SIGNAL AMPLITUDE VERSUS STRESS FOR NAS 537-8P-128 BUSHING THERMALLY FITTED INTO 7075 ALUMINUM CYLINDER

5937

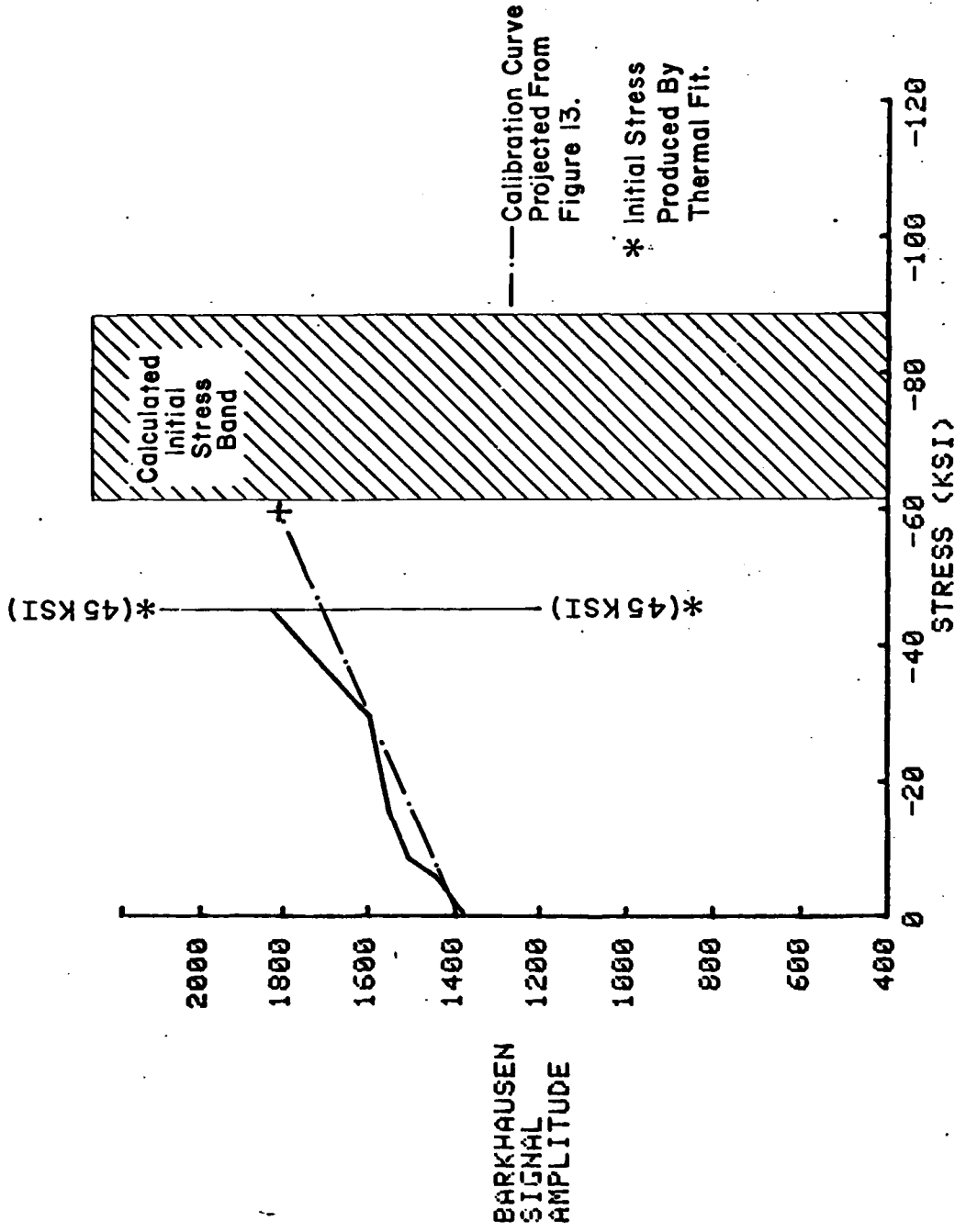
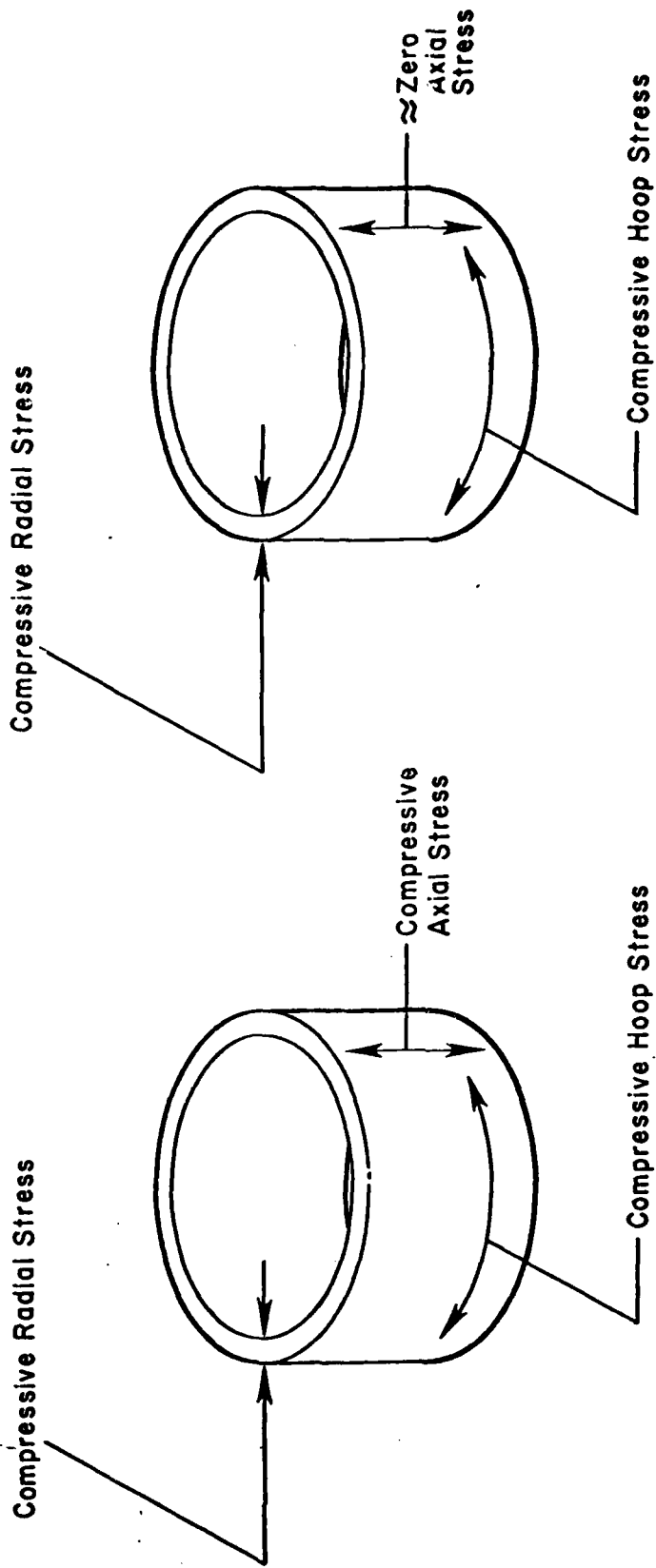


FIGURE 20. AVERAGE BARKHAUSEN SIGNAL AMPLITUDE VERSUS STRESS FOR NAS 537-12P-56 BUSHING THERMALLY FITTED INTO 7075 ALUMINUM CYLINDER



Thermal Interference Fit

Clamping Fixture

FIGURE 21. COMPARISON OF MAJOR STRESSES PRODUCED IN A STEEL BUSHING BY A THERMAL INTERFERENCE FIT AND MAJOR STRESSES PRODUCED BY THE CLAMPING FIXTURE

The Barkhausen probe was positioned to be most sensitive to the hoop stress in the bushing, but high stress levels in other directions may effect the Barkhausen signal amplitude. Thus, the scatter in the Barkhausen signal data obtained in this experiment could be due to variable axial stress. A second possible cause for the inconsistent results of this experience could be the difficulty of assembling these rather tight thermal fits at the specified temperatures.

VI. CONCLUSIONS

The Barkhausen measurements on bushings as a function of applied hoop stress showed good sensitivity and repeatability when the existing residual stresses in the bushing are taken into account. While the relationship of Barkhausen signal amplitude to hoop stress for actual thermal fit bushings also showed encouraging results but was less predictable. Thus, it is concluded, although some questions remain unresolved, the Barkhausen Noise Analysis method offers potential in determining whether the desired stress level have been achieved in bushings assembled used thermal interference fits.

VII. RECOMMENDATIONS

It is recommended that additional data be taken on test specimens which have been assembled by the supplier of the drag struts. This will insure that the same process is used to assemble the specimens as is used on the actual drag strut. Secondly, it is recommended that a special Barkhausen probe be fabricated to allow accurate repositioning on the actual drag strut bushings without special fixturing.

Using this special probe, data would be taken on actual drag struts to evaluate the process of making Barkhausen measurements on the actual part and to develop a simple procedure for making the inspection. This would set the stage for the Barkhausen stress measurement procedure to be integrated in to inspect production parts.

REFERENCES

1. Donaldson, W. L. and Pasley, R. L., "A New Method of Nondestructive Stress Measurements," Proceedings of the Sixth Symposium on Nondestructive Evaluation of Aerospace and Weapon Systems Components and Materials, Western Periodicals Co., Los Angeles, 1967, pp. 563-575.
2. Bray, F. H. and Fitz III, H. H., "Development and Qualification of a Magnetic Technique for the Nondestructive Measurement of Residual Stress in CH-47A Rotor Blade Spars," American Helicopter Society, Preprint No. 752, May, 1973.
3. Gardner, C. G., "Engineering Evaluation of Barkhausen Effect Stress Measurement Instrumentation for Application to Autofrettaged Gun Tubes," Final Report, Contract No. DAAG-46-72-C-0111, Army Materiel and Mechanics Research Center, Watertown, Massachusetts, September, 1972. Unpublished.
4. Barton, J. R. and Kusenberger, F. N., "Residual Stresses in Gas Turbine Engine Components from Barkhausen Noise Analysis," Paper 74-GT-51, ASME Gas Turbine Conference, Zurich, Switzerland, April, 1974.
5. Bloch, R. J., "Application of Portable Magnetic Equipment to the Nondestructive Determination of Stress in Ferromagnetic Material," Presented at the Symposium on Advanced Nondestructive Testing Techniques, Army Materiel and Mechanics Research Center, Watertown, Massachusetts, 1-3 June 1971. To be published in Int. J. Nondestructive Testing.
6. Gardner, C. G., Matzkanin, G. A., and Davidson, D. L., "The Influence of Mechanical Stress on Magnetization Processed and Barkhausen Jumps in Ferromagnetic Materials," Int. J. Nondestructive Testing, 3, pp. 131-169 (1971).
7. Gardner, C. G., and Matzkanin, G. A., "Barkhausen Jumps in Plastically deformed Silicon-Iron," AIP Conference Proceedings No. 5, Ed. by C. O. Graham, Jr. and J. J. Rhyne, AIP, New York, pp. 1509-1513, 1972.

8. Birdwell, J. A. and Barton, J. R., "Development and Application of Barkhausen Instrumentation Concepts for Measuring Stress in Ferromagnetic Steels," Final Report, Contract No. N00156-71-C-0362, Naval Air Engineering Center, Philadelphia, Pennsylvania, September, 1971, Unpublished.
9. Matzkanin, G. A. and Burkhardt, G. L., "Advanced Signal Analysis and Instrumentation for Barkhausen Stress Measurement in Steels," Final Report, Contract No. DAAG-46-76-C-0028, Army Materiels and Mechanics Research Center, Watertown, Massachusetts, September, 1977.
10. Barkhausen H., "Zwei mit Hilfe der Neuen Verstarker Entdeckte Erscheinungen," Physik, Z. 20, pp. 401-403 (1919).
11. W. D. Perry and J. R. Barton, "Development of evaluation Equipment for the Measurement of Residual Stress in Aircraft Components" Final Report, Contract No. DAA J01-76-C-0663 (P60), U.S. Army Aviation System Command, St. Louis, Missouri, August, 1977.
12. J. H. Faupel "Designing for Shrink Fits" Machine Design, January 1954.

APPENDIX A

CALCULATION OF HOOP STRESS

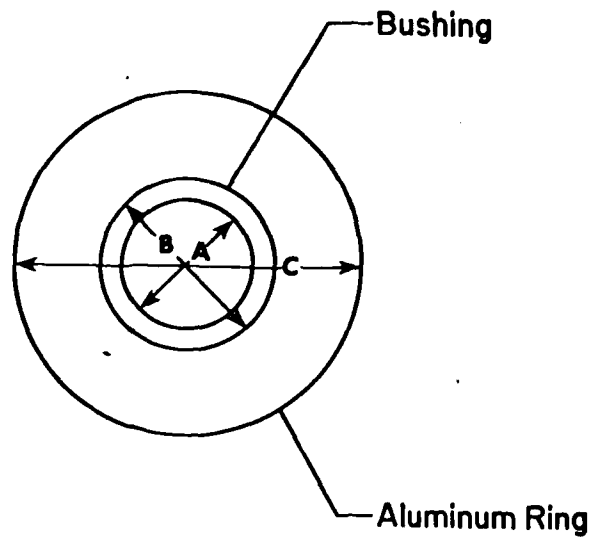
PRODUCED BY A THERMAL INTERFERENCE FIT

CALCULATION OF HOOP STRESS
PRODUCED BY A THERMAL INTERFERENCE FIT

The basic equations used for this calculation are from a paper titled "Designing for Shrink Fits" by J. H. Fawpel. For the bushing hoop stress calculations, the equations utilized were based on the following situation:

1. Different Materials
2. Different Yield Strengths
3. Hollow Shaft

Figure A-1 is a definition of variables utilized in the computer program to calculate the maximum hoop stress in the bushing and the maximum hoop stress in the aluminum as a function of dimensional interference between the aluminum and the bushing at 75°F. Figure A-2 is a listing of the computer program. The program language is "BASIC". Figure A-3 shows the results of the computation for a NAS537-12P bushing mounted in a 1.90" diameter aluminum ring.



- A - Inside diameter of Bushing
- B - Outside diameter of Bushing
- C - Outside diameter of Aluminum Ring
- D - Dimensional Interference at 75°F
- I - Dimensional Interference at 75°F times 1000
- K - Scratch Variable
- K_1 - Scratch Variable
- K_2 - Scratch Variable
- R - Scratch Variable
- S - Maximum stress in Bushing
- T - Maximum stress in Aluminum
- U_1 - Poisson's Ratio for Steel
- U_2 - Poisson's Ratio for Aluminum

FIGURE A1 - DEFINITION OF VARIABLES

```

LIST
99 INIT
100 DIM D(20),S(20),T(20)
110 REM:MOD. FOR ALUMINUM
120 E1=1.04E+7
130 REM:MOD. FOR STEEL
140 E2=2.9E+7
150 PRINT "ENTER BUSHING, I.D., BUSHING O.D., ALUMINUM O.D."
160 INPUT A,B,C
165 PRINT " BUSHING I.D. ",A," BUSHING O.D.",B," AL. O.D.",C
170 REM:POISSON RATIO FOR ALUMINUM
180 U1=0.33
190 REM: POISSON RATIO FOR STEEL
200 U2=0.3
210 K1=((B↑2+C↑2)/(C↑2-B↑2)+U1)/E1
220 K2=((A↑2+B↑2)/(B↑2-A↑2)-U2)/E2
230 K=K1+K2
240 PRINT " J INTERFERENCE", "BUSHING STRESS (PSI)", "ALUM. STRESS(PSI)"
250 FOR I=1 TO 10 STEP 0.5
260 D(I)=I*1.0E-3
270 R=D(I)/(B*K)
280 S(I)=2*R*B↑2/(B↑2-A↑2)
290 T(I)=R*B↑2/(C↑2-B↑2)*(1+C↑2/B↑2)
300 PRINT D(I),S(I),"",T(I)
310 NEXT I
320 GO TO 100

```

FIGURE A-2. LISTING OF COMPUTER PROGRAM TO CALCULATE HOOP STRESSES.


```

RUN
ENTER BUSHING, I.D., BUSHING O.D., ALUMINUM O.D.
.734, .9393, 1.900
BUSHING I.D. 0.734
BUSHING O.D. 0.9393
AL. O.D. 1.9

```

```

INTERFERENCE
1.0E-3
0.0015
0.0025
0.0035
0.0045
0.0055
0.0065
0.0075
0.0085
0.0095
0.01
ENTER BUSHING, I.D., BUSHING O.D., ALUMINUM O.D.

BUSHING STRESS (PSI)
16717.8298944
25076.7448417
33435.6597889
41794.5747361
50153.4896933
58512.4046305
66871.3195777
75230.234525
83589.1494722
91948.0644194
100306.979367
108665.894314
117024.809261
125383.724208
133742.639156
142101.554103
150460.46905
158819.383997
167178.298944

ALUM. STRESS (PSI)
5360.09146501
8040.13719751
10720.18293
13400.2286625
16080.274395
18760.3201275
21440.36586
24120.4115925
26800.457325
29480.5030576
32160.5487901
34840.5945226
37520.6402551
40200.6859876
42880.7317201
45560.7774526
48240.8231851
50920.8689176
53600.9146501

```

FIGURE A-3. RESULTS OF THE COMPUTATION FOR A NAS537-12 BUSHING

ATE
LMED
8